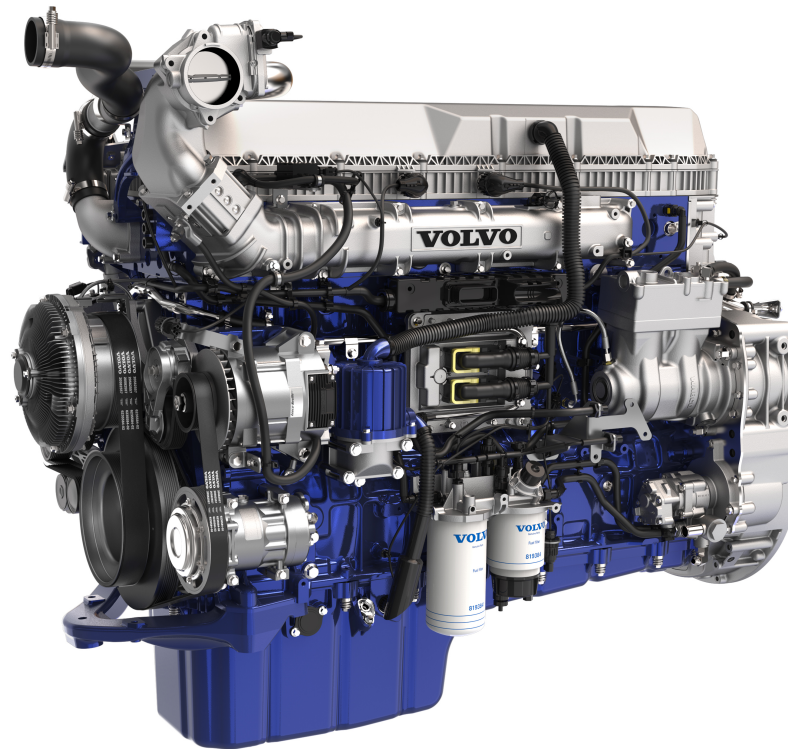




**CHALMERS**  
UNIVERSITY OF TECHNOLOGY

---



# Torque estimation from in-cylinder pressure sensor for closed loop torque control

Systems, Control and Mechatronics

PER-SEBASTIAN PETTERSSON  
ANTON KJELLIN



MASTER'S THESIS EX051/2017

# Torque estimation from in-cylinder pressure sensor for closed loop torque control

PER-SEBASTIAN PETTERSSON  
ANTON KJELLIN



**CHALMERS**  
UNIVERSITY OF TECHNOLOGY

Department of Signals and Systems  
*Division of Systems and Control*  
Automatic control  
CHALMERS UNIVERSITY OF TECHNOLOGY  
Gothenburg, Sweden 2017

Torque estimation from in-cylinder pressure sensor for closed loop torque control  
PER-SEBASTIAN PETTERSSON  
ANTON KJELLIN

© PER-SEBASTIAN PETTERSSON & ANTON KJELLIN, 2017.

Supervisor: Johan Engbom, Volvo Group Truck Technology  
Examiner: Torsten Wik, Department of Signals and Systems

Master's Thesis EX051/2017  
Department of Signals and Systems  
Division of Systems and Control  
Automatic Control  
Chalmers University of Technology  
SE-412 96 Gothenburg  
Telephone +46 31 772 1000

Cover: Volvo Trucks D13 engine. Source: Volvo Group Trucks Technology

Typeset in L<sup>A</sup>T<sub>E</sub>X  
Gothenburg, Sweden 2017

Torque estimation from in-cylinder pressure sensor for closed loop torque control  
PER-SEBASTIAN PETTERSSON & ANTON KJELLIN  
Department of Signals and Systems  
Chalmers University of Technology

## Abstract

In-cylinder pressure sensors are gradually moving out of the laboratory and into production type engines, thus making more direct information of the combustion process available for the engine control unit.

For several reasons it is important to accurately control the torque produced by the engine. In light of this objective, this thesis propose and studies two methods for estimating the average indicated torque of a heavy duty diesel engine with measurements from a single in-cylinder pressure sensor. It is further studied how this estimate can be used as feedback in a torque control loop.

For this case study, it is demonstrated that the angular precision when sampling the cylinder pressure is very important for the accuracy of the estimation but that the sampling interval can be moderate and still produce a compelling estimation. Furthermore, it is demonstrated that the sensor drift, characteristic for piezo-electric in-cylinder pressure sensors, could be neglected when estimating the torque.

In an engine cell test it is illustrated how the influence from faulty injectors on the output torque could be corrected, by using the estimation of the average indicated torque as feedback.

Keywords: In-cylinder pressure sensor, combustion control, torque control, ECU, EMS, ECM, torque estimation.



## Acknowledgements

When performing this work, we took help and guidance from some excellent people, who deserve our greatest gratitude. First we want to say thank you to Johan Engbom at Volvo for his enthusiasm and commitment in our project. We would also like to thank our supervisor professor Torsten Wik at Chalmers for his guidance and assistance.

Deepest gratitude is also due to Ph.D. Marcus Hedegård at Chalmers, without whose knowledge and assistance this study would not have been successful.

Conny Nicander at Volvo deserves our greatest appreciation for supporting our project.

Thanks also to Kedar Jaltare and Viktor Andersson for giving us good technical guidelines throughout numerous consultations.

Many others have made valuable and inspirational suggestions which have improved our work greatly, Igor Lumpus, Mikael Svensson, Bengt Lassesson, Arash Idelchi and others.

Anton Kjellin and Per-Sebastian Pettersson, Gothenburg, June 2017



# Contents

<b>1</b>	<b>Introduction</b>	<b>1</b>
1.1	Thesis purpose and scope . . . . .	2
1.2	Thesis outline . . . . .	2
<b>2</b>	<b>System overview</b>	<b>5</b>
2.1	Angular measurement . . . . .	5
2.2	In-cylinder pressure sensor . . . . .	6
<b>3</b>	<b>Torque estimation methods</b>	<b>7</b>
3.1	Estimation method 1: Riemann sum . . . . .	9
3.2	Estimation method 2: Tailor made basis . . . . .	9
<b>4</b>	<b>Estimation method analysis</b>	<b>11</b>
4.1	Data set . . . . .	11
4.1.1	Reference indicated torque . . . . .	12
4.2	Expected error introduced when using only one ICPS . . . . .	13
4.3	Design parameters Estimation method 1 . . . . .	14
4.4	Design parameters Estimation method 2 . . . . .	17
4.5	Pressure measurement offset impact analysis . . . . .	20
4.6	Angle measurement offset impact analysis . . . . .	21
4.7	Discussion . . . . .	22
<b>5</b>	<b>Controller</b>	<b>25</b>
<b>6</b>	<b>Implementation and lab set-up</b>	<b>29</b>
6.1	Engine control unit implementation . . . . .	29
6.2	Engine test cell set-up . . . . .	30
<b>7</b>	<b>Results</b>	<b>31</b>
7.1	Torque estimation . . . . .	31
7.2	Closed loop torque controller 1 . . . . .	33
7.3	Closed loop torque controller 2 . . . . .	35
<b>8</b>	<b>Discussion</b>	<b>37</b>
8.1	Estimators . . . . .	37
8.2	Controllers . . . . .	38
<b>9</b>	<b>Conclusion</b>	<b>39</b>
<b>10</b>	<b>Future Work</b>	<b>41</b>
10.1	Gather reference data and analyze error . . . . .	41
10.2	Adaptive reference feed forward controller . . . . .	41

10.3 Individually weighting cylinder contributions . . . . .	41
10.4 Investigating impact of crankshaft torsion on estimation accuracy . .	42
<b>Bibliography</b>	<b>43</b>
<b>A Appendix 1</b>	<b>I</b>

# Notation

## *Abbreviations*

ECM	Engine Control Module
GTT	(Volvo) Group Trucks Technology
ICPS	In-Cylinder Pressure Sensor
TDC	Top Dead Center

## *Capital Letters*

$C$	Constant value
$E$	Torque error
$F$	Controller, Transfer function
$F_{LP}$	Moving average filter, Transfer function
$G$	Plant, Transfer function
$L$	Crank lever function scaled by cylinder area
$\mathbf{L}$	Vector with pre-calculated values from crank lever function
$N_c$	Number of cylinders
$N_f$	Order of filter
$T$	Torque [Nm]
$T_0$	Operating point (Nm, RPM)
$T_f$	Friction torque [Nm]
$T_g$	Indicated/gas torque [Nm]
$T_g^*$	Reference gas torque [Nm]
$T_m$	Mass torque [Nm]

*Small Letters*

$b$	Piston diameter [m]
$e$	Error
$e_r$	Control error
$f_\theta$	Sample frequency [samples/degree]
$\mathbf{k}$	Optimized vector of constants
$l$	Length of connecting rod [m]
$\tilde{\mathbf{p}}$	Vector of pressure measurements [Pa]
$p_0$	Crank case pressure, approximated to ambient pressure [Pa]
$p_d$	Pressure drift [Pa]
$p_{Ex}$	Exhaust pressure [Pa]
$p_g$	Effective pressure, difference between cylinder and crankcase [Pa]
$p_i$	Cylinder pressure for cylinder $i$ [Pa]
$p_I$	Intake manifold pressure [Pa]
$p_{max}$	Expected maximum pressure [Pa]
$r$	Distance from crankshaft to connecting rod
$s$	Vertical piston position [m]
$\tilde{\mathbf{y}}$	Vector of measured weights for Estimation method 2
$z$	Frequency domain argument

*Greek Letters*

$\alpha$	Crank angle offset [degree]
$\theta$	Crank shaft angle relative to TDC [degree]
$\theta_i$	Crank angle where samples are taken [degree]
$\theta_I$	Vector of crank angles where samples are taken [degree]
$\Omega_i$	Function relating flywheel angle to cylinder individual angle for cylinder $i$
$\Theta$	4-stroke engine cycle angular interval $[0^\circ, 720^\circ)$ .
$ \Theta $	Length of the 4-stroke engine cycle, $720^\circ$ .
$\psi_j$	Scalar valued basis function
$\Lambda_{j,l,m}$	Matrix with spline parameters
$n_\phi$	Number of parameters in Estimation method 2
$\gamma$	Value that represent the contribution to the mean indicated torque from a sub-interval
$\omega$	Engine speed [rad/s]
$\bar{\omega}$	Mean engine speed [rad/s <sup>2</sup> ]
$\rho$	Pearson linear correlation coefficient

*Diacritical marks*

$\sim$	Measurement
$\hat{\phantom{x}}$	Approximation or estimate
$\bar{\phantom{x}}$	Average value

# 1 | Introduction

New alternative bio fuels have started to enter the market and engine manufacturers are seeing a future where their engines will need to be able to run effectively on several different fuels. The properties between these fuels may differ substantially. For example, a difference in energy content between diesel and biodiesel of 7% is common[11]. Together with a continued need to improve engine efficiency and reduce vehicle emissions, for environmental reasons and stricter government regulations, better and more refined combustion control is of great importance [13].

The conventional control of heavy duty diesel engines is based on feed-forward of sensor information of what enters and leaves the combustion chamber. The various control signals are determined using pre-calibrated look-up tables, basically making the control an open-loop structure. The time and resources required for calibration are significant and grows exponentially with the increase of control parameters[16]. However, in case the fuel properties are not what the engine has been calibrated to, or the engine components have changed, the behavior of the engine will differ from what is intended, and from what is optimal.

Engine manufacturers are therefore moving towards including more closed loop control structures where the quantity that is to be controlled is measured, either directly or indirectly. An advantage of closed loop control is also that it inherently requires less calibration.

## **In-cylinder pressure**

With a few exceptions, for example knock control, the closed loop control structures that has been suggested for combustion control relies heavily on information about the in-cylinder pressure[8][10][12][17]. The in-cylinder pressure is a fundamental variable in both thermodynamics and classical mechanics, and it is possible to extract a lot of other quantities from it, such as heat release, torque, peak-pressure position and exhaust composition[1][3].

Until now few of these methods have been implemented into production type engines. The main reason for this is that the in-cylinder pressure sensors (ICPS) have, until recently, been considered too expensive and fragile and therefore limited to research use only. This has, parenthetically, triggered a research field where methods to estimate the cylinder pressure from other sensors have been studied e.g. by combining crankshaft acceleration and torque measurements [2][6][13]. Recent advancement in sensor technology, now makes it sensible for engine manufactures to include ICPS in their production types engines. Accurate measurements of the pressure from each combustion cycle provides many new opportunities for advanced feedback control and it has been shown that a reduction in both emissions and improved fuel efficiency is possible[17].

## Torque control

One of the variables that could be extracted from the in-cylinder pressure is the indicated torque (gas torque),  $T_g$ , which is the torque that is created by the pressure difference between the cylinder and the crankcase acting on the piston. The gas torque is the biggest contributor to the output torque,  $T$ , from the crankshaft

$$T = T_g - T_f - T_m. \quad (1.1)$$

The friction torque,  $T_f$ , and the mass torque,  $T_m$ , imposed by the piston assembly are the other contributing factors.

The mathematical basis for computing the indicated torque from the cylinder pressure is a geometric relationship that can be derived from the geometry of the mechanical linkage between the piston and the crankshaft (Chapter 3). If an algorithm could be derived for production type engine control modules it would be possible to give a live in-vehicle estimate of the indicated torque. This estimate could be used in a feedback control structure, making it possible to keep engine behavior even though fuel or engine properties changes.

### 1.1 Thesis purpose and scope

The purpose of this thesis is to evaluate if a torque controller that uses a live estimate of the average indicated torque, based on measurement from only one ICPS, as feedback is feasible to introduce into production type engines from Volvo Trucks.

The available computational power and memory of the engine control unit is scarce. To introduce a new function or sensor it is therefore necessary that the computational complexity of the function and the required sample frequency of the sensor is reasonable. It is also necessary that the function gives reliable output, i.e. the function needs to be robust against possible disturbances.

### 1.2 Thesis outline

In this thesis two methods for estimating the average indicated torque, using an ICPS from one cylinder, are formulated, analyzed and compared. Two feedback torque controllers are also formulated and analyzed. A live test is then presented where the methods have been implemented on a production type engine control module and verified in an engine test cell at Volvo Group Trucks Technology.

Chapter 2 contains an overview of the system with its sensors, actuators and other components.

In Chapter 3 the two methods for estimating the mean indicated torque are formulated and described. Based on a large data-set containing previous measured cylinder pressure curves and other engine parameters the methods are analyzed with regards to sample frequency, sensor drift, crank angle resolution and robustness to measurement noise. This is described in Chapter 4.

The two controllers are presented and derived in Chapter 5. The first controller is a simple integrating controller with a feed-forward of the reference. The second

is an extension of the first where a dynamic look-up table that is populated by the integrated error from different operating points is introduced.

The implementation of the estimation methods and controllers on the engine control unit later used in the live test is briefly described in Chapter 6. This chapter also contains information about how the measurements were taken during the live test.

Chapter 7 contains the result from the live test done on a 13 litre 6 cylinder heavy duty diesel engine from Volvo.

The last chapters contains a discussion, presents the conclusions drawn from the work described and presents proposed future work.



## 2 | System overview

Diesel engines are compression ignited engines. This means that the fuel injected into the combustion chamber is ignited only by high compression. The torque output is controlled by controlling the air and fuel entering the combustion chamber. This is in contrast to gasoline engines where the fuel is ignited by a spark plug and where also the ignition needs to be controlled .

The control of the engine is handled by one central unit called the engine control module (ECM). The ECM is connected to several sensors fitted to the engine and its surroundings, for diagnose and control. The sensors used in this thesis, in addition to the ICPS, are the exhaust pressure sensor, the intake manifold pressure sensor, the ambient pressure sensor and the angle measurement sensors. These are standard sensors used in production type engines.

### 2.1 Angular measurement

For several reasons it is important for the ECM to know the current orientation of the crankshaft. The crank shaft angle,  $\theta$ , is detected at discrete points on the flywheel and the ECM estimates the angle between these points by extrapolation based on the engine speed. Another detection point on the cam shaft together with missing measurement points on the flywheel, referred to as missing teeth, are used to find the absolute angle. On the engine considered in this thesis there is a detection point each  $6^\circ$  and three gaps separated by  $120^\circ$ . Figure 2.1 illustrates the detection points on the flywheel.



**Figure 2.1:** *Illustration of the detection points on the flywheel. The gaps (missing teeth) of detection points that are used to establish absolute position are also illustrated. The engine considered in this project have three of these gaps, separated by 18 teeth.*

## 2.2 In-cylinder pressure sensor

The cylinder pressure,  $p_i(\theta)$ , is measured by an in-cylinder pressure sensor. An typical ICPS is illustrated in Figure 2.2. The sensor is placed in the cylinder head with the tip directly exposed to the combustion gas pressure. Some different technologies are used, such as piezo-electric, piezo-resistive and optical pressure sensing.

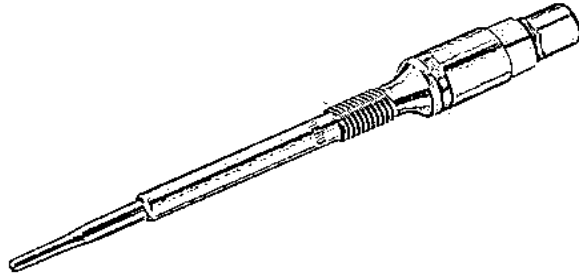


**Figure 2.2:** *Combustion chamber pressure sensor. Is fitted in the cylinder with the tip directly exposed to the combustion gas pressure.*

In this thesis a flush mounted piezo-electric sensor from the manufacturer Kistler is used. The central component in a Piezo-electric pressure sensor is the quartz crystal that generates a charge when exposed to pressure. If the pressure is kept constant the charge will eventually leak to zero. Piezo-electric pressure sensors can therefore only measure dynamic pressures, i.e changing pressures, as opposed to static pressures. Another property of piezo-electric sensors is that the measurement signal drifts over time.

### 3 | Torque estimation methods

Figure 3.1 depicts the mechanical linkage between the piston and the crankshaft. Pressure in the cylinder produces a force on the piston which is transmitted, via the connecting rod, to the crankshaft and results in a torque.

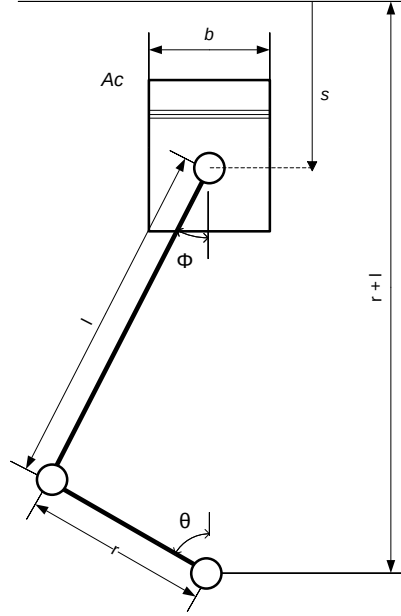


**Figure 3.1:** *Piston-crankshaft mechanical linkage.*

The relationship between pressure and the indicated torque for cylinder  $i$  is

$$T_{g,i}(\theta) = L(\theta)p_{g,i}(\theta) \quad (3.1)$$

where  $p_{g,i}(\theta)$  is the pressure difference between the combustion chamber and the crankcase, i.e.  $p_{g,i}(\theta) = p_i(\theta) - p_0$ . The pressure in the crankcase,  $p_0$ , can be approximated to atmospheric pressure [4].

$L(\theta)$  states the relation

$$L(\theta) = A_c \frac{ds}{d\theta}, \quad (3.2)$$

where  $A_c = \frac{b^2}{4}\pi$  is the piston area and  $\frac{ds}{d\theta}$  is the crank lever function [4]

$$\frac{ds}{d\theta} = r \sin(\theta) \left( 1 + \frac{r}{l} \frac{\cos(\theta)}{\sqrt{1 - \frac{r^2}{l^2} \sin^2(\theta)}} \right), \quad (3.3)$$

which relates force on the piston to torque on the crankshaft.

The indicated torque at the output side of the crankshaft,  $T_g(\theta)$ , is a sum of contributions from the  $N_c$  individual cylinders, i.e.

$$T_g(\theta) = \sum_{i=1}^{N_c} T_{g,i}(\theta) = \sum_{i=1}^{N_c} L(\Omega_i(\theta))p_{g,i}(\theta), \quad (3.4)$$

### 3. Torque estimation methods

---

where  $\Omega_i(\theta)$  is cylinder individual angle for cylinder  $i$  at flywheel angle  $\theta$ . The cycle average indicated torque at the output side of the crankshaft is

$$\bar{T}_g = \frac{1}{|\Theta|} \int_{\Theta} T_g(\theta) d\theta = \sum_{i=1}^{N_c} \frac{1}{|\Theta|} \int_{\Theta} L(\Omega_i(\theta)) p_{g,i}(\Omega_i(\theta)) d\theta \quad (3.5)$$

where  $\Theta = [0^\circ, 720^\circ)$  is the 4-stroke engine cycle and  $|\Theta| = 720^\circ$  is the length of the cycle.

Assuming periodicity in  $\theta$  of all pressure signals at steady state operation, i.e.  $p_{g,i}(\theta) = p_{g,i}(\theta + |\Theta|)$ , then

$$\bar{T}_g = \sum_{i=1}^{N_c} \frac{1}{|\Theta|} \int_{\Theta} L(\Omega_i(\theta)) p_{g,i}(\Omega_i(\theta)) d\theta_i := \sum_{i=1}^{N_c} \bar{T}_{g,i}. \quad (3.6)$$

Using weights,  $w_i$ , relating the torque contribution from cylinder  $i$  to that of one cylinder,  $x$ , the total average indicated torque can be expressed in terms of one measured pressure,  $p_{g,x}(\theta)$  as

$$\bar{T}_g = \sum_{i=1}^{N_c} w_i \bar{T}_{g,x} \quad (3.7)$$

Algorithms using momentaneous engine speed measurements to calculate the weights have been developed with promising results [5]. In this thesis however, it has been assumed that the angle-pressure relationship in all cylinders are equal, i.e.  $w_i = 1 \forall i$ , and therefore

$$\bar{T}_g = N_c \bar{T}_{g,x} = \frac{N_c}{|\Theta|} \int_{\Theta} L(\theta) p_{g,x}(\theta) d\theta. \quad (3.8)$$

Further, when approximating the pressure inside the crankcase,  $p_0$ , to atmospheric pressure it can be considered constant on the time scale of one engine cycle. Then the contribution from  $p_0$  cancels, i.e.

$$\bar{T}_g = \frac{N_c}{|\Theta|} \int_{\Theta} L(\theta) (p_x(\theta) - p_0) d\theta = \frac{N_c}{|\Theta|} \left( \int_{\Theta} L(\theta) p_x(\theta) d\theta - p_0 \underbrace{\int_{\Theta} L(\theta) d\theta}_{=0} \right). \quad (3.9)$$

That is, assuming equal angle-pressure relationship in all cylinders and constant pressure inside the crankcase during the engine cycle, the average indicated torque can be expressed as

$$\bar{T}_g = \frac{N_c}{|\Theta|} \int_{\Theta} L(\theta) p_x(\theta) d\theta, \quad (3.10)$$

using pressure measurements from only on cylinder,  $x \in [1, N_c]$ .

### 3.1 Estimation method 1: Riemann sum

The first method considered to approximate the integral in Equation (3.10) is a Riemann middle sum. The continuous pressure signal,  $p(\theta)$ , will be sampled in  $\theta$  with frequency  $f_s = \frac{n}{|\Theta|}$  [samples/degree]. The system will thus have access to the pressure signal at  $n$  angle-equidistant points,  $\theta_i$ , over the cycle and  $\bar{T}_g$  will be estimated using this data according to

$$\bar{T}_g \approx \hat{\bar{T}}_g = N_c \frac{1}{n} \sum_{i=0}^{n-1} L(\theta_i) \tilde{p}(\theta_i), \quad (3.11)$$

with  $\theta_i = (2i + 1) \frac{|\Theta|}{2n}$ .

Once the number of samples,  $n$ , and  $\theta_I := \{\theta_i : i = 1, \dots, n\}$  have been decided  $\frac{N_c}{n} L(\theta_i)$  can be pre-calculated and collected in a column vector,  $\mathbf{L} := \frac{N_c}{n} L(\theta_I)$ . The average indicated torque can then be computed from the scalar product

$$\hat{\bar{T}}_g = \mathbf{L}^T \tilde{\mathbf{p}}, \quad (3.12)$$

where  $\tilde{\mathbf{p}} := \tilde{p}(\theta_I)$  is a column vector of measurements.

### 3.2 Estimation method 2: Tailor made basis

In [2] it was assumed that cylinder pressure on a given operating region can be modelled as

$$\hat{p}(\theta) = \underbrace{[\psi_0(\theta), \dots, \psi_{n_\phi}]}_{\psi(\theta)} \tilde{\mathbf{y}} \quad (3.13)$$

where  $\psi_j$  are scalar valued basis functions in angle  $\theta$  and  $\tilde{\mathbf{y}} = [1, \tilde{y}_1, \dots, \tilde{y}_{n_\phi}]$  is a vector of corresponding weights that are individual for each pressure curve. For identification of  $\psi_j$  a large set of measured pressured curves were used, and  $\psi_j$  was parameterized using cubic splines, i.e.

$$\psi_j(\theta) = \sum_{m=0}^3 \theta^m \Lambda_{j,l,m}, \quad (3.14)$$

where  $\Lambda_{j,l,m}$  are the spline parameters. It was also shown that the weights  $\tilde{y}_j$ ,  $j = 0, \dots, n_\phi$  can be chosen as cylinder pressures at distinct angles. Using this, a convex optimization problem for the spline parameters,  $\Lambda_{j,l,m}$ , in the model could be formulated. It was further suggested to choose some of the weights in  $\tilde{\mathbf{y}}$  to be other measured quantities. Evaluation for the same engine as in the current study showed that as few as  $n_\phi = 6$  measured parameters gave good accuracy over a selected operating region.

The above suggests that the average gas torque could be estimated to a satisfactory accuracy by a linear mapping from only a few measured parameters. Explicitly, we have

$$\bar{T}_g \approx \hat{\bar{T}}_g = \frac{1}{|\Theta|} \int_{\Theta} L(\theta) \hat{p}(\theta) d\theta = \frac{1}{|\Theta|} \int_{\Theta} L(\theta) \psi(\theta) d\theta \tilde{\mathbf{y}} := \mathbf{k}^T \tilde{\mathbf{y}} \quad (3.15)$$

### 3. Torque estimation methods

---

that is

$$\widehat{T}_g = \mathbf{k}^T \widetilde{\mathbf{y}}, \quad (3.16)$$

where

$$\mathbf{k}^T = \frac{1}{|\Theta|} \int_{\Theta} L(\theta) \psi(\theta) d\theta \quad (3.17)$$

is a constant vector.

This method of estimation may require less data to be sampled and processes than Estimation method 1. If this estimate is also accurate and robust then this method may be preferred.

For determination of  $\mathbf{k}$  a set of  $N_p$  pressure curves measured under different conditions within a specified operating region are used. An optimization problem is then formulated as a least squares problem, i.e

$$\min_{\mathbf{k}} \mathbf{e}^T \mathbf{e}, \quad (3.18)$$

where  $\mathbf{e}$  is the model error

$$\mathbf{e} = \overline{\mathbf{T}}_g - \widehat{\mathbf{T}}_g = \begin{bmatrix} \overline{T}_{g,1} \\ \vdots \\ \overline{T}_{g,N_p} \end{bmatrix} - \begin{bmatrix} \widetilde{\mathbf{y}}_1^T \\ \vdots \\ \widetilde{\mathbf{y}}_{N_p}^T \end{bmatrix} \mathbf{k} := \overline{\mathbf{T}}_g - \mathbf{A}\mathbf{k}, \quad (3.19)$$

where  $T_{g,i}$  is taken as the best possible approximation of the true torque calculated using high frequency sampled data and where row  $i$  in  $A$  collects measurements from the  $i$ :th pressure curve. The unconstrained solution to (3.18) is found as [7]

$$\nabla_{\mathbf{k}} \mathbf{e}^T \mathbf{e} = \mathbf{0} \Rightarrow \mathbf{k} = (\mathbf{A}^T \mathbf{A})^{-1} \mathbf{A}^T \overline{\mathbf{T}}_g \quad (3.20)$$

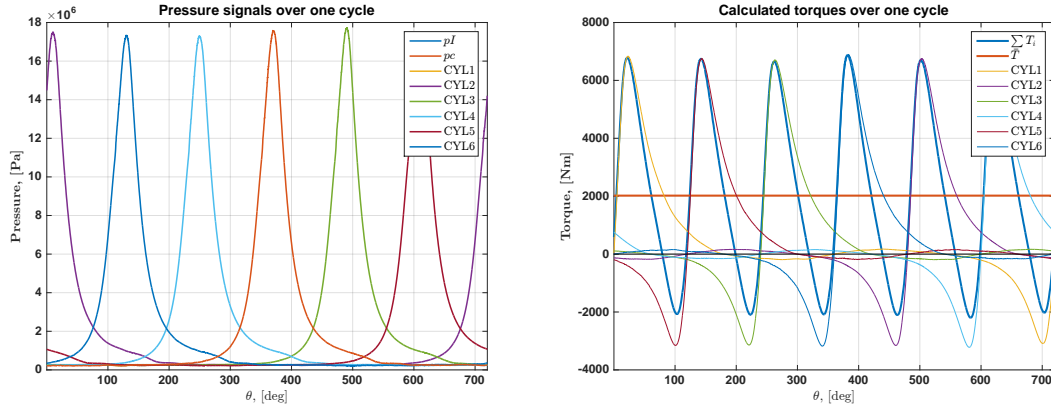
# 4 | Estimation method analysis

Both methods for estimating the average indicated torque presented above have design parameters that affect the precision and computational complexity of the estimation algorithms. A provided data-set taken from the intended engine type is used in this chapter to analyze different choices of parameters. Further, the expected effect of different possible error sources on the estimation algorithms are also studied.

## 4.1 Data set

Analysis and testing of the estimation methods have been based on a large data-set collected from a 13 liter engine in a test cell at Volvo Trucks. The data collected includes pressure and angle measurements sampled in time with high frequency at different operating points  $T_0$  (load and speed). Also included are measurements of the atmospheric pressure, pressure in the intake manifold and crank shaft angle. Table A.1 in Appendix A lists information about the data set.

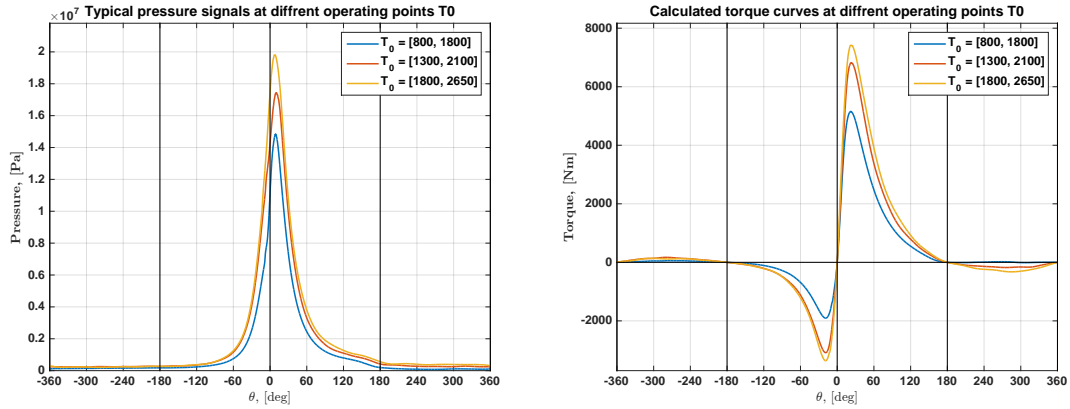
The data set includes pressure measurements from all 6 cylinders. Typical individual pressure signals and calculated torque signals over one engine cycle are shown in Figure 4.1. Figure 4.2 shows selected pressure measurements and indicated torque from one cylinder at different operating points.



(a) *Pressure measurements.*

(b) *Corresponding calculated torque*

**Figure 4.1:** *Individual signals from all cylinders over one engine cycle.*



(a) Pressure measurements.

(b) Corresponding calculated torque signals.

**Figure 4.2:** Signals from one ICPS over one cycle at different operating points.

### 4.1.1 Reference indicated torque

To evaluate the precision of the two estimation methods a reference mean indicated torque is needed. This reference should, as far as possible, represent the true physical indicated torque.

The high frequency sampled pressure data in the data set is distorted by high frequency noise. The signal is sampled with at least  $3.4 * 10^3$  samples per cycle. All information in the continuous pressure signal up to a frequency of  $1.7 * 10^3$  repetitions per cycle will therefore be represented in the sampled signal. The continuous pressure signal seems to be practically band limited to 750 repetitions per cycle and all frequency content above this limit is considered as high frequency noise, either from the measurement or the process. A low pass filtered pressure signal with cut-off frequency of 750 repetitions per cycle is considered the best possible representation of the physical continuous pressure signal available and is used to calculate the reference mean indicated torque.

Figure 4.3 shows pressure measurement data and the low pass filtered signal at three different operating points. The magnitude of the noise is fairly constant over the cycle except for angles around TDC. This may be actual high frequency pressure variations in the cylinder but considered as process noise and attenuated by filtering.

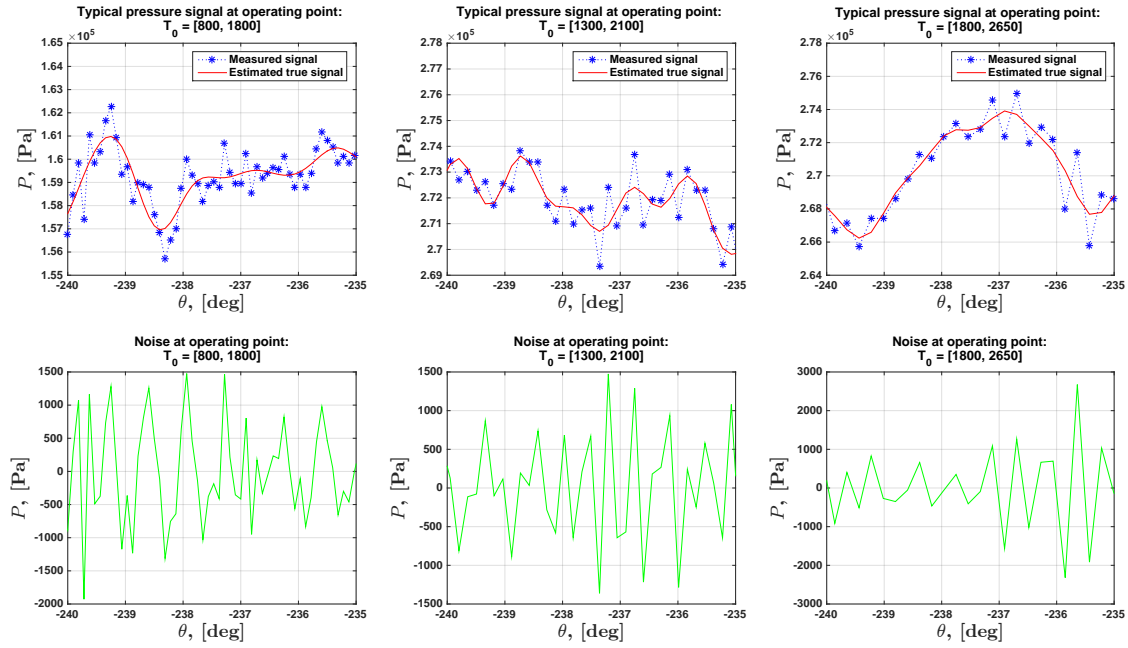


**Figure 4.3:** Pressure samples and low pass filtered signals at the three operating points considered. Zoomed on flat intake stroke

Reference torque is calculated from the low pass filtered high frequency sampled data as a Riemann middle sum, the error of the reference using all data is then limited by [15]

$$E_{max} = \frac{N_c |\Theta|^2}{24n^2} \left( \frac{1}{n} \sum_{i=1}^n |T_g''|_{max,i} \right) \quad (4.1)$$

Approximating the second derivative of a typical torque signal calculated from low pass filtered pressure measurements,  $|T_g''|$ , an estimate of  $E_{max}$  is calculated. From this calculation it is shown that the error in the calculated reference at an operating point with the lowest angular sampling frequency in the data set ( $f_\theta \geq 4.74$ ) is smaller than 0.2 Nm.

## 4.2 Expected error introduced when using only one ICPS

In order to use only one ICPS it has been assumed that the contribution to the average torque from all individual cylinders are equal. The validity of this assumption is examined on the data-set. The relative error for the average indicated torque introduced by this assumption,

$$e_{i,h} = \frac{6\bar{T}_{g,i} - \sum_{j=1}^6 \bar{T}_{g,j}}{\sum_{j=1}^6 \bar{T}_{g,j}} \quad (4.2)$$

when using measurements from cylinder  $i \in [1, 6]$  at operating point  $h$  is presented in Figure 4.4. Here the average value over the complete test cycle has been used.

The magnitude of the largest relative error found is for cylinder 1 at the operating point  $T_0 = [1800, 1800]$  where the contribution is on average around 5% off.

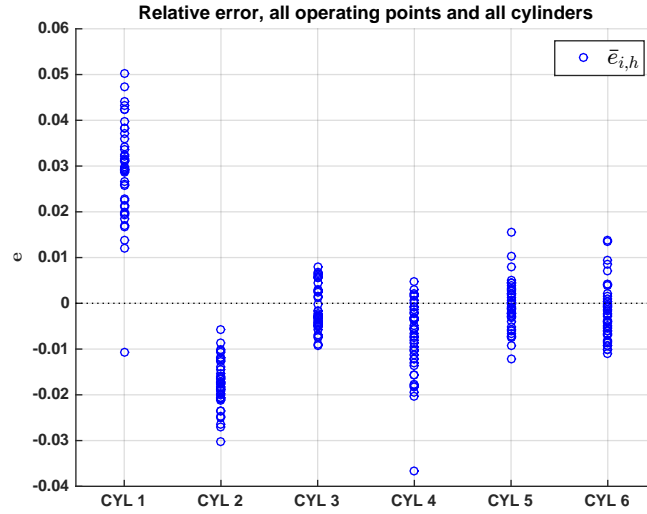


**Figure 4.4:** *Relative offset of individual cylinder contributions to the mean torque.*

### 4.3 Design parameters Estimation method 1

The parameter to be chosen for Estimation method 1 is  $\theta_I$  in Equation (3.12). Equidistant sampling symmetric around TDC is assumed, thus the choice of  $\theta_I$  is fully determined by choice of sampling frequency,  $f_\theta = \frac{n}{|\Theta|}$ , where  $n$  is the number of samples per engine cycle. The computational demand is proportional to  $f_\theta$  and the expected error in the approximation is also affected by the choice of  $f_\theta$ .

This section investigates how the error stemming from approximating the integral by a sum and error stemming from pressure measurement noise is impacted by choice of  $f_\theta$ .

**Numerical integration error** Figure 4.5 displays the resulting error stemming from approximating the integral by a sum, as a function of sampling frequency for three operating points selected to cover the speed and torque span of the data set. This suggests that the sample interval can be moderate and still produce an accurate estimate. For sampling frequencies higher than  $\frac{1}{18}$  [samples/degree] the error is well below 1%.

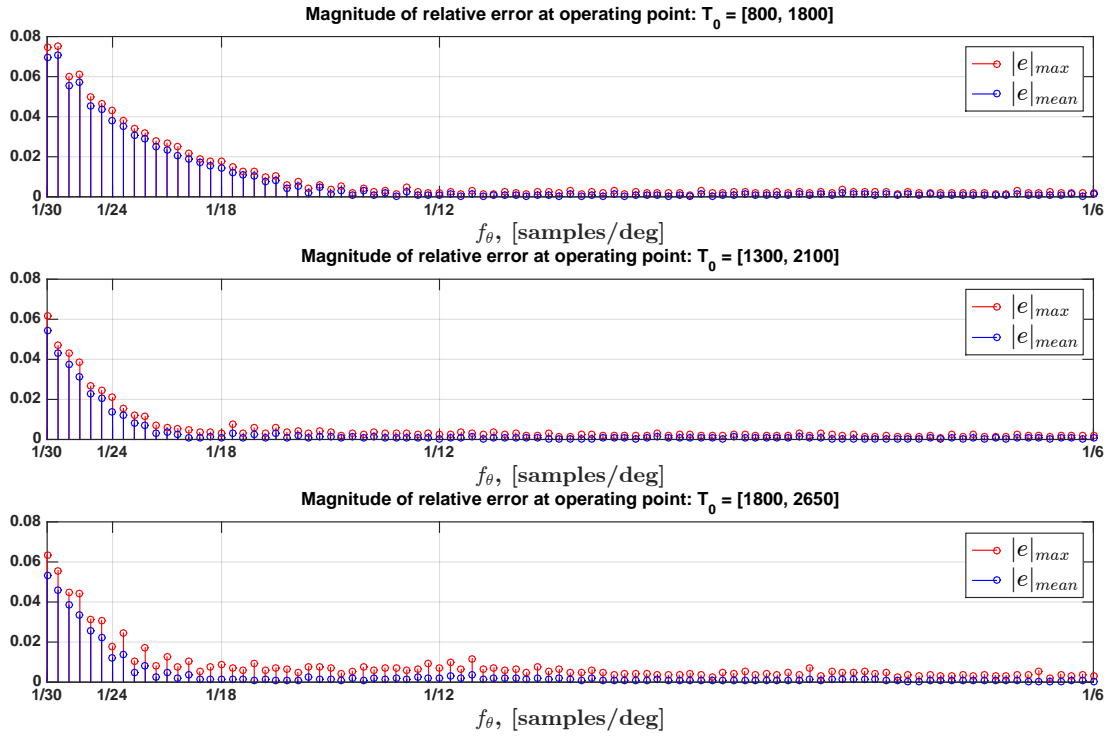


Figure 4.5: Magnitude of relative error from data over  $f_\theta$ .

**Pressure noise error** The measured pressure signal,  $\tilde{p}(\theta)$ , carries information of the actual pressure,  $p(\theta)$ , distorted by high frequency measurement and process noise,  $e$ .

$$\tilde{p}(\theta) = p(\theta) + e \quad (4.3)$$

The impact of the noise on the mean torque estimate using Estimation method 1 can be analyzed

$$\hat{\bar{T}}_g = N_c \frac{1}{n} \sum_{i=1}^n L(\theta_i) \tilde{p}(\theta_i) = N_c \frac{1}{n} \sum_{i=1}^n L(\theta_i) p(\theta_i) + N_c \frac{1}{n} \sum_{i=1}^n L(\theta_i) e = \bar{T}_g + E, \quad (4.4)$$

where  $E$  is the resulting error,  $E = \frac{N_c}{n} \sum_{i=1}^n L(\theta_i) e$ . If  $e$  is gaussian,  $e \sim \mathcal{N}(\mu(\tilde{p}), \sigma^2(\tilde{p}))$ , then  $E \sim \mathcal{N}(\mu_E, \sigma_E^2)$  where

$$\begin{aligned} \mu_E &= \frac{N_c}{n} \sum_{i=1}^n L(\theta_i) f_\mu(\tilde{p}(\theta_i)), \text{ and} \\ \sigma_E^2 &= \frac{N_c^2}{n^2} \sum_{i=1}^n L^2(\theta_i) f_\sigma^2(\tilde{p}(\theta_i)). \end{aligned} \quad (4.5)$$

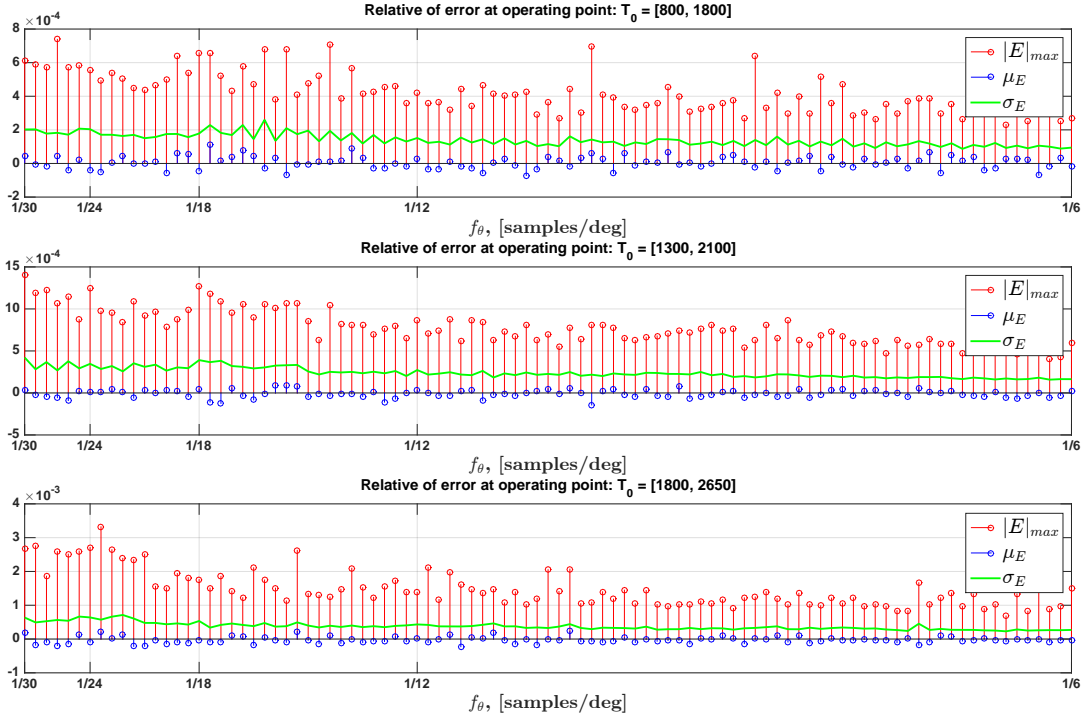
If  $e$  has zero mean,  $f_\mu(\tilde{p}) = 0$ , and constant variance,  $f_\sigma^2(\tilde{p}) = \sigma_e^2$ , then

$$\begin{aligned} \mu_E &= 0, \text{ and} \\ \sigma_E^2 &= \frac{N_c^2 \sigma_e^2}{n^2} \sum_{i=1}^n L^2(\theta_i) \end{aligned} \quad (4.6)$$

#### 4. Estimation method analysis

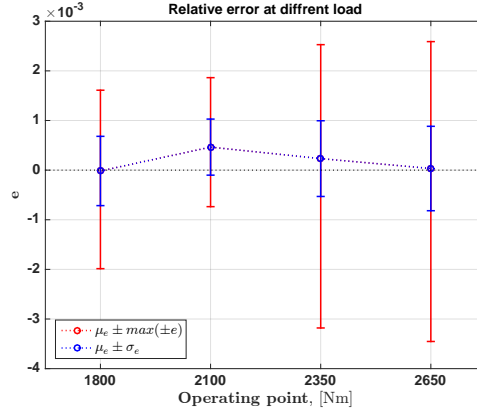
and  $\sigma_E^2$  is proportional to  $n^{-1}$ .

Figure 4.6 shows the mean, the standard deviation and the maximum of the error the pressure measurement noise in the data set contributes with,  $E$ . The maximal error increases with decreasing sampling frequency but even at sampling frequencies as low as  $\frac{1}{30}$  [samples/degree] the maximal error found is well below 1%.



**Figure 4.6:** Max and mean noise contribution over sampling frequency,  $f_\theta$ .

**Total error** Clearly the total error decrease with an increase in sampling frequency. The target environment limits the maximum tractable sampling frequency, Figure 4.7 shows the total error using the same data as above with  $n = 120$ . The maximum error found is below 0.5%



**Figure 4.7:** Total relative estimation error with  $f_\theta = \frac{120}{|\Theta|}$  at different operating points.

## 4.4 Design parameters Estimation method 2

The parameter to be selected for Estimation method 2 is  $\tilde{\mathbf{y}}$  in Equation (3.16).

The process in the cylinder is very different over the different engine strokes and it can thus be expected that measurements have different impact on the different strokes. It makes sense to partition the cycle accordingly into 4 non-overlapping sub-intervals,  $I_h$ ,  $h \in [1, 4]$ , and evaluate parameters separately for the different strokes, i.e.

$$\bar{T}_g = \frac{1}{|\Theta|} \sum_{h=1}^4 \int_{I_h} L(\theta) p(\theta) d\theta := \sum_{h=1}^4 \bar{T}_{g,h}. \quad (4.7)$$

From Equation (3.16) we have

$$\hat{\bar{T}}_g = \sum_{h=1}^4 \mathbf{k}_h^T \tilde{\mathbf{y}}_h = \mathbf{k}^T \tilde{\mathbf{y}} \quad (4.8)$$

and then  $\mathbf{k}^T = [\mathbf{k}_1^T, \dots, \mathbf{k}_4^T]$ ,  $\tilde{\mathbf{y}}^T = [\tilde{\mathbf{y}}_1^T, \dots, \tilde{\mathbf{y}}_4^T]$ .

Studying typical pressure curves a partition of the engine cycle is made according to Table 4.1.

$h$	Stroke	$I_h$	$\gamma_h \approx$	Simplistic pressure model
1	Compression	$[-180^\circ, -20^\circ)$	0.2266	$p(\theta)V(\theta) = c,$ $p(-180) = p_I$
2	Work	$[-20^\circ, 140^\circ)$	0.7148	-
3	Exhaust	$[140^\circ, 360^\circ)$	0.0277	$p(\theta)V(\theta) = n(\theta)Rt,$ $\frac{dn}{dt} = k(p(\theta) - p_{Ex})$
4	Intake	$[360^\circ, 540^\circ)$	0.0309	$p(\theta) = p_I$

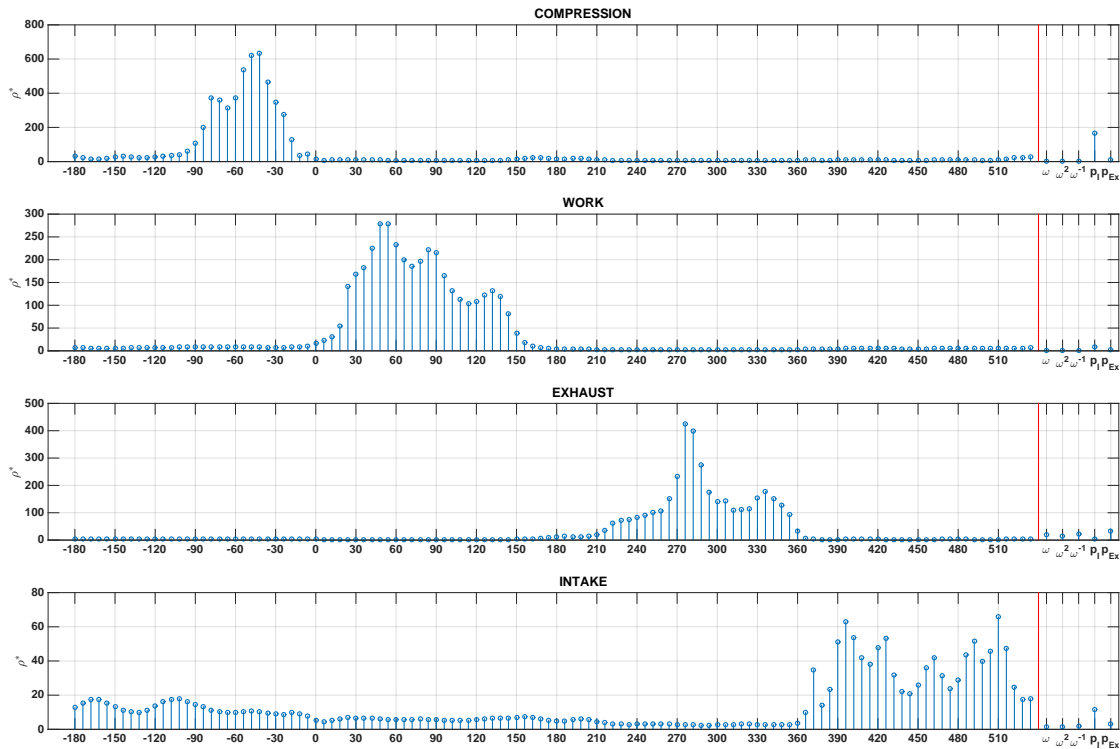
**Table 4.1:** Partition of engine cycle into strokes.

Table 4.1 also list  $\gamma_h = |\bar{T}_{g,h}| \left( \sum_{h=1}^4 |\bar{T}_{g,h}| \right)^{-1}$ , a measure of the strokes contribution to the total gas torque and simplistic pressure models for the different strokes,

#### 4. Estimation method analysis

indicating what parameters may be of importance.

Possible choices of measured parameters include in-cylinder pressure ( $p(\theta)$ ) at angles  $\theta = 6n$ , average engine speed over the cycle ( $\bar{\omega}$ ), intake manifold pressure ( $p_I$ ), exhaust manifold pressure ( $p_{Ex}$ ) and functions of those. Parameters that exhibit strong linear correlation to the sought quantity can be expected to perform better. Figure 4.8 shows  $\rho^* = \frac{1}{1-|\rho|}$  where  $\rho \in [-1, 1]$  is the Pearson correlation coefficient [9] for selected possible parameters. This measure is used to compare the parameters linear correlation to the mean indicated stroke torque.



**Figure 4.8:** Comparison of selected parameters linear correlation to measured mean indicated torque over the different engine strokes. The first 120 parameters are measured pressures at 6 degree interval over the engine cycle. The last 5 are, in order from left to right,  $\bar{\omega}$ ,  $\bar{\omega}^2$ ,  $\bar{\omega}^{-1}$ ,  $P_I$ ,  $P_{Ex}$ .

For each stroke 4 combinations ( $\tilde{\mathbf{y}}_h = [\tilde{d}_1]^T$ ,  $\tilde{\mathbf{y}}_h = [\tilde{d}_2]^T$ ,  $\tilde{\mathbf{y}}_h = [\tilde{d}_1, \tilde{d}_2]^T$  and  $\tilde{\mathbf{y}}_h = [\tilde{d}_1, \tilde{d}_2, \tilde{d}_3]^T$ ) of 3 reasonable parameters ( $\tilde{d}_i$ ) have been evaluated.  $\tilde{d}_i$  was for each stroke chosen, based on result presented in Figure 4.8, as

$h$	$d_1$	$d_2$	$d_3$
1	$p_I$	$p(-42^\circ)$	$p(-48^\circ)$
2	$p(54^\circ)$	$p(84^\circ)$	$p(48^\circ)$
3	$p_{Ex}$	$p(276^\circ)$	$p(336^\circ)$
4	$p(396^\circ)$	$p(510^\circ)$	$p(402^\circ)$

**Table 4.2:** Parameters chosen for estimation for each stroke,  $\tilde{\mathbf{y}}_h$  (cells marked gray indicates parameters used in the final optimization - result over full cycle presented in figure 4.9).

For each combination an optimal  $\mathbf{k}_h$  have been calculated using part of the data set, this  $\mathbf{k}_h$  and another part of the data set have then been used to evaluate the particular choice of parameters. Table 4.3 lists the mean (black), the standard deviation (blue) and the maximal magnitude (red) of the relative error (Equation (3.19)) for each stroke and all chosen combinations of parameters.

$h$	$\tilde{\mathbf{y}}_h = d_1$	$\tilde{\mathbf{y}}_h = d_2$	$\tilde{\mathbf{y}}_h = [d_1, d_2]$	$\tilde{\mathbf{y}}_h = [d_1, d_2, d_3]$
1	-0.0004	-0.0003	-0.0003	-0.0004
	0.0159	0.0089	0.0090	0.0087
	0.0697	0.0309	0.0311	0.0320
2	-0.0001	-0.0006	-0.0003	-0.0003
	0.0120	0.0122	0.0113	0.0112
	0.0283	0.0371	0.0310	0.0282
3	0.4075	-0.0393	-0.0450	-0.0270
	11.4285	0.6775	0.7851	0.8358
	322.7999	14.2170	18.6255	15.4270
4	-0.0006	-0.0065	-0.0020	-0.0015
	0.0469	0.0504	0.0297	0.0282
	0.1575	0.2931	0.1009	0.0789

**Table 4.3:** Error-properties of approximation of stroke average torque using different  $\tilde{\mathbf{y}}_h$  for all strokes,  $h = 1 \dots 4$  (cells marked gray indicates parameters used in the final optimization - result over full cycle presented in figure 4.9).

Table 4.4 lists the same error properties for the approximation of the total average torque over the full cycle, Equation 4.8, for a selected set of interesting combinations  $\tilde{\mathbf{Y}}_{i_1 i_2 i_3 i_4}^T = [\tilde{y}_1^T, \tilde{y}_2^T, \tilde{y}_3^T, \tilde{y}_4^T]$ .  $i_h$  in  $\tilde{\mathbf{Y}}_{i_1 i_2 i_3 i_4}^T$  gives the number of parameters used for stroke  $h$ , when  $i_h = 1$  the best choice between  $\tilde{d}_1$  and  $\tilde{d}_2$  in terms of smallest maximum error is chosen (total number of parameters used is given by  $\sum_{\forall h} i_h$ ).

$\tilde{\mathbf{Y}}_{3333}$	$\tilde{\mathbf{Y}}_{3322}$	$\tilde{\mathbf{Y}}_{2222}$	$\tilde{\mathbf{Y}}_{2321}$	$\tilde{\mathbf{Y}}_{1212}$	$\tilde{\mathbf{Y}}_{2121}$	$\tilde{\mathbf{Y}}_{1111}$
-0.0004	-0.0005	-0.0005	-0.0006	-0.0006	-0.0003	-0.0003
0.0148	0.0149	0.0158	0.0164	0.0163	0.0181	0.0183
0.0488	0.0436	0.0432	0.0463	0.0403	0.0487	0.0489

**Table 4.4:** Error-properties of approximation of total average torque over full cycle using different  $\tilde{\mathbf{Y}}_{i_1 i_2 i_3 i_4}^T = [\tilde{y}_1^T, \tilde{y}_2^T, \tilde{y}_3^T, \tilde{y}_4^T]$ .

The smallest maximal magnitude of the error is achieved for  $\widetilde{\mathbf{Y}}_{1212}$ , column 5 (marked gray) using in total 6 parameters. What parameters are used is given by cells marked gray in Table 4.2.

Figure 4.9 shows the mean, the standard deviation and the maximum and minimum relative error of the total approximation over different operating points using  $\mathbf{k}^T = [\mathbf{k}_1^T, \mathbf{k}_2^T, \mathbf{k}_3^T, \mathbf{k}_4^T]$  corresponding to  $\widetilde{\mathbf{Y}}_{1212}$ . The magnitude of the biggest error found using this  $\mathbf{k}$  on the data-set is smaller than 5%.

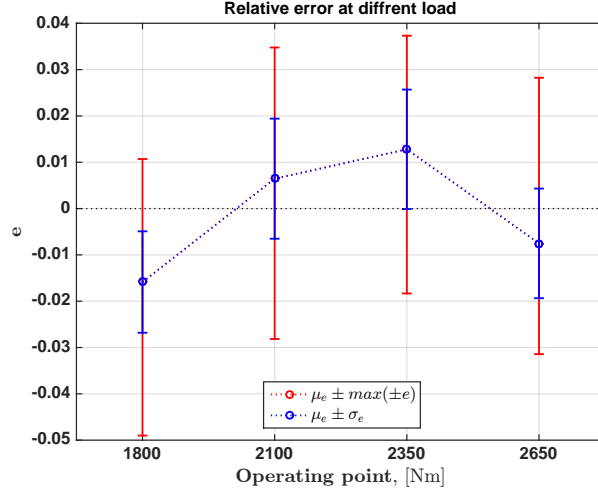


**Figure 4.9:** Estimation results of full engine cycle at different operating points.

## 4.5 Pressure measurement offset impact analysis

Piezo-electric pressure sensors drift over time, inducing an additive measurement error,  $p_d(t)$ , to the pressure measurements. The drift is slow and can therefore be considered constant,  $p_d(t) \approx C$ , over each engine cycle. The pressure measurements over an engine cycle,  $\tilde{p}(\theta)$ , will thus include this error

$$\tilde{p}(\theta) = p(\theta) + C. \quad (4.9)$$

Since  $L(\theta)$  is an odd periodic function with fundamental period  $\Theta$ ,

$$\int_{\Theta} L(\theta) d\theta = 0. \quad (4.10)$$

When adding a constant error to Equation (3.11)

$$\widehat{T}_g = \frac{N_c}{n} \sum_{i=0}^{n-1} L(\theta_i) (p_g(\theta) + C) = \underbrace{\frac{N_c}{n} \sum_{i=0}^{n-1} L(\theta_i) p_g(\theta)}_{\overline{T}_g} + \underbrace{\frac{N_c}{n} C \sum_{i=0}^{n-1} L(\theta_i)}_{\overline{T}_d} \quad (4.11)$$

it becomes evident that the sensor drift can be neglected in the computation for Estimation method 1 if the number of samples is large,

$$\overline{T}_d = \frac{N_c}{n} C \sum_{i=0}^{n-1} L(\theta_i) \xrightarrow{n \rightarrow \infty} 0. \quad (4.12)$$

Further, if the samples are taken symmetrically around TDC ( $L(\theta)$  being an odd function around TDC) then  $\bar{T}_d = 0$  for any number of samples used.

This is also verified by simulations on data. Figure 4.10 displays the magnitude of the relative error induced by pressure measurement offsets over  $p_d(t) \in [0, 0.1p_{max}]$ , where  $p_{max}$  is the expected maximal cylinder pressure.

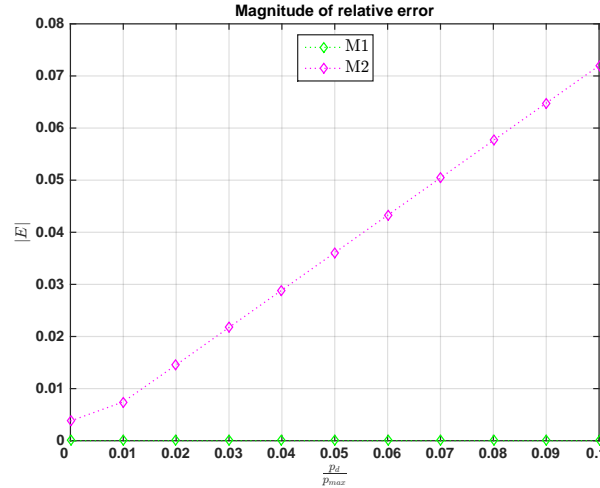


**Figure 4.10:** Relative error from constant pressure offset for Estimation method 1 (M1), and Estimation method 2 (M2).

Clearly Estimation method 1 is very robust to pressure measurement offset. The error induced in Estimation method 2 grows approximately linearly with the drift and is substantial. When using Estimation method 2, compensation for sensor drift is needed.

## 4.6 Angle measurement offset impact analysis

The crank shaft angle is measured at discrete points on the flywheel (60 points), see Figure 2.1. A angle measurement offset could arise if for example the sensor is fitted wrongly or if there is a constant time lag present in the sampling. The effect of such an error will be investigated for both estimation methods based on data.

Adding an offset,  $\alpha$ , to the angular measurements gives  $T_g(\theta, \alpha) = p_g(\theta)A_p \frac{ds}{d\theta}(\theta + \alpha)$  and

$$\bar{T}_g(\alpha) = \frac{N_c}{|\Theta|} \int_{\Theta} p_g(\theta)A_p \frac{ds}{d\theta}(\theta + \alpha)d\theta. \quad (4.13)$$

The relative magnitude of the induced error is expressed as

$$E(\alpha) = \left| \frac{\bar{T}_g(\alpha)}{\bar{T}_g(0)} - 1 \right| \quad (4.14)$$

Figure 4.11 shows the resulting torque error over angular offset for Estimation methods 1 and 2. The result demonstrates that angular precision in the pressure sampling

#### 4. Estimation method analysis

is very important for accurate estimation. For example, an offset of  $1^\circ$  yields an error of almost 10%.

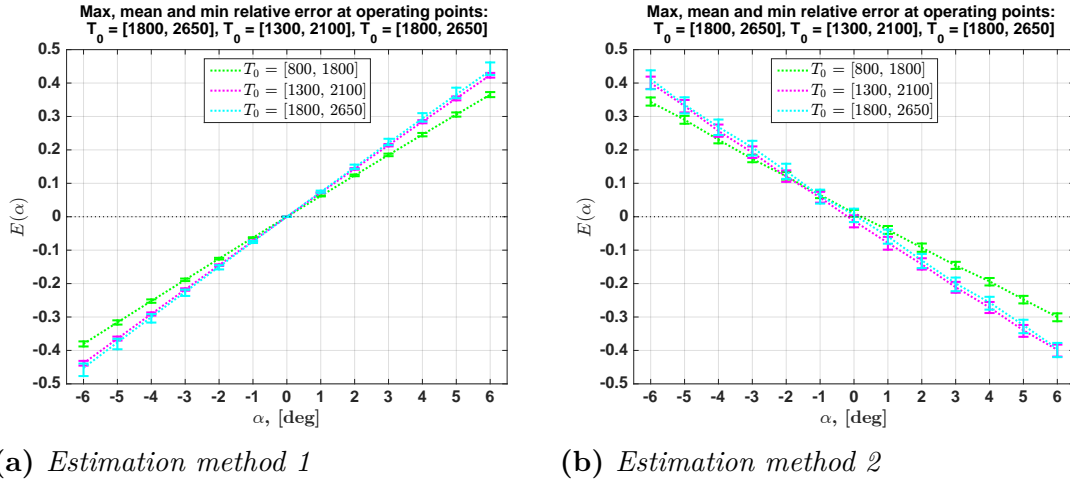


**Figure 4.11:** Magnitude of relative error of torque estimation over angular measurement offset.

### 4.7 Discussion

Comparing the resulting total error of the two estimation methods, Figure 4.7 (Estimation method 1,  $n = 120$ ) and Figure 4.9 (Estimation method 2), clearly Estimation method 1 with  $n = 120$  outperforms Estimation method 2. Figure 4.12 presents a comparison of the total relative error of the two estimation methods over sampling frequency of Estimation method 1. With  $n \geq 30$  the maximum recorded error using Estimation method 1 is smaller than that of Estimation method 2.

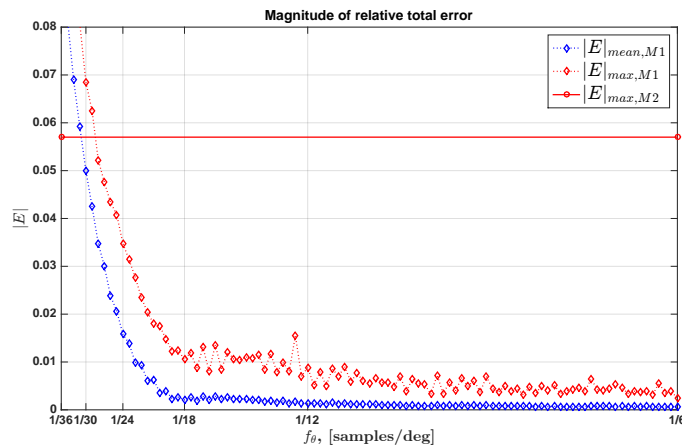


**Figure 4.12:** Comparing the total relative error of Estimation method 1 ( $M1$ ) at different sampling frequency to that of Estimation method 2 ( $M2$ ).

It is clear that the expected error induced from using only one ICPS is substantial, see Figure 4.4. The robustness to measurement offset analysis conducted showed

that the two methods are comparably robust to angular offset and that Estimation method 1 performs superior when pressure offset is present.

The computational demand for both estimation methods is proportional to the number of measurements used. However, Estimation method 2 also needs an algorithm to compensate for the sensor drift.



## 5 | Controller

Over time properties of the engine fuel system affecting the factory calibration might change. For example worn injectors or a change of fuel type could introduce a torque error,  $T_{error}$ , in the conventional open loop control structure. In this section it is assumed that the mean indicated torque,  $\bar{T}_g$ , can be measured and a feedback loop could be included. Using standard control theory and the z-transform, the current system is first modeled as a discrete system with a discrete sampling interval of one engine cycle.

The current control structure goes through a chain of different steps which starts with the torque demand from the pedal and ends with opening times for the fuel injectors. The idea is to insert a closed loop controller into this structure. The controller will thus have a torque reference as input and another torque reference as output.

**System model** A model that relates the torque reference from the pedal,  $T_g^*$ , to the actual mean indicated torque,  $\bar{T}_g$  is derived.

The pedal demand is fetched at some point in the engine cycle and the injector timing for the cycle is calculated and applied. The indicated torque output is related to the amount of fuel injected. Thus the system from torque reference to the actual indicated torque from cycle to cycle can be viewed as static, i.e there is no dynamic (time step dependent) behaviour present. The system can thus be modelled as a constant, equal to one assuming perfect calibration.

With conventional feed-forward control the relationship between the torque reference and the actual average indicated torque for each engine cycle is then assumed to be

$$\bar{T}_g = T_g^* + T_{error} + T_{noise}, \quad (5.1)$$

where  $T_{noise} \sim \mathcal{N}(0, \sigma^2)$  is white noise which is included to capture the fact that there will always be small random and thus non-controllable variations in the combustion between each engine cycle.

**Control design** With a direct estimation of the indicated torque it is possible to extend the conventional controller with a feedback loop that can compensate for  $T_{error}$ . To handle the random variations it is necessary to filter the measured signal to remove  $T_{noise}$ . The optimal filter to remove a Gaussian noise is a moving average filter [14]

$$F_{LP}(z) = \frac{1}{N} \sum_{i=0}^{N_f} z^{-i}.$$

The drawback with the moving average filter is that it introduces a delay. The torque reference,  $T_g^*$ , is therefore also fed through the same filter in order for the control error,  $e_r$ , to make sense. The complete system is illustrated in Figure 5.1.

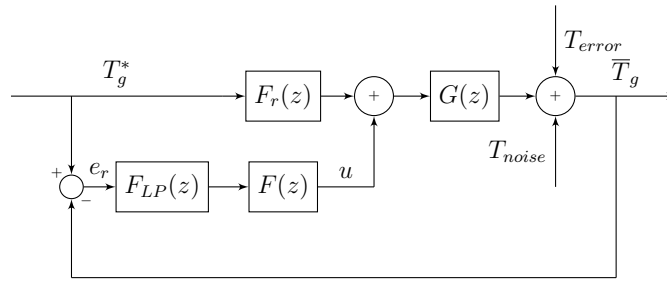


**Figure 5.1:** Illustration of the control structure.

The torque output for the complete system when  $G(z) = 1$  and direct feed forward is used,  $F_r(z) = 1$ , becomes

$$\bar{T}_g = T_g^* + \frac{1}{1 + F_{LPF}F}(T_{error} + T_{noise})$$

**Controller 1: I-controller** The first controller,  $F_1(z)$ , is a conventional I-controller. A time delay ( $z^{-1}$ ) will have to be included in order to capture limitations of the scheduling in the engine control unit.

$$F_1(z) = K_i \frac{z^{-1}}{1 - z^{-1}} \cdot \frac{1}{z}.$$

The system can be explicitly written as

$$\bar{T}_g = T_g^* + \frac{1 - z^{-1}}{1 - z^{-1} + \frac{K_i}{N_f} \sum_{i=2}^{N_f+2} z^{-i}} (T_{error} + T_{noise}). \quad (5.2)$$

The stability of the system depends on the order of the filter,  $N_f$ , and the control constant,  $K_i$ . A simulation of the system output with  $T_{error} = 200$  Nm,  $T_{noise} \sim \mathcal{N}(0, 5)$  and  $N_f = 6$  is illustrated in Figure 5.2 for different  $K_i$ .

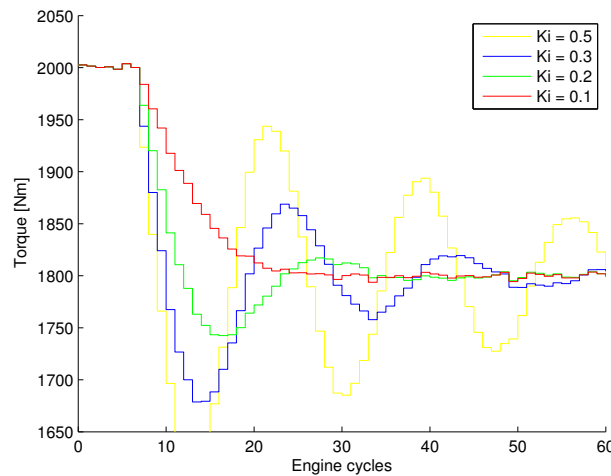


**Figure 5.2:** Output for different  $K_i$ , constant offset error and  $N_f = 6$ .

**Controller 2:** Worn injectors or changing fuel qualities will likely produce an error proportional to the demanded torque output. Further this type of error will be fairly constant (change very slowly) over time considering the time scale of engine cycles. Therefore a torque dependent controller may better (faster) follow a changing torque reference.

One way to implement such a controller is to divide the engine torque range into bins and introduce a vector containing the control signal at torque reference values represented by the bins. The control signal is computed by torque reference dependent interpolation in this vector and using I-control as in the case of controller 1. The vector is updated based on the error at reference values in the bin range and is thus a function of historic errors in this range.

Essentially this results in several I-controllers, in this case each with equal  $K_i$ , operating in a more narrow torque range and activated as a mode switch with a moving torque reference. Interpolation in the vector is used to give smooth operation. Figure 5.3 illustrates the function of controller 2,  $F_2(z)$  interacts with the surrounding system as in Figure 5.1.

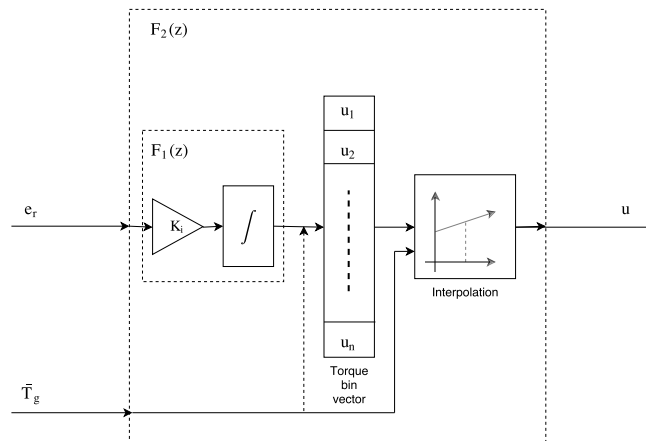


**Figure 5.3:** *Illustration of Controller 2.*



# 6 | Implementation and lab set-up

This chapter gives an explanation on how the estimators and controller were implemented on the production type engine control module. It also describes the lab set-up used in the test cell to generate the results which are described in Chapter 7.

## 6.1 Engine control unit implementation

The programming of the engine control unit is divided into two layers. The low level layer is called the platform layer and the high level layer, where the estimators and controller mainly operates, is called the application layer. The implementation of functions in the application layer is done in Simulink with a software for automatic code generation, based on a subset of Simulink models and blocks, called TargetLink.

The control unit estimates the angle of the crankshaft based on the sensors described in Section 2.1. Functions in the control unit can therefore be executed either on an angular basis or a time basis. Figure 6.1 gives an overview of how the functions have been implemented and how they relate to each other.

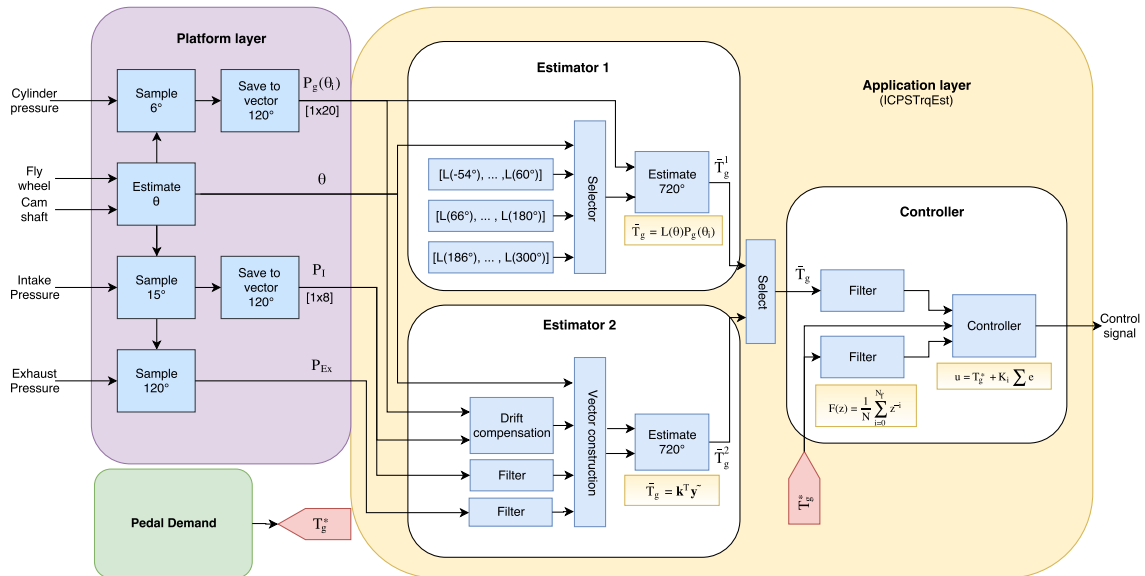


**Figure 6.1:** Illustration of how the function have been implemented in the engine control module.

**Platform layer** The platform layer takes samples of the cylinder pressure at specified angles of the crankshaft, every sixth degree, and saves these in a vector. This vector is then forwarded to the application layer three times each crankshaft revolution, i.e every 120th degree. The functions in the application layer are scheduled to run synchronized with the forwarding of the pressure vector, also every 120th degree. The intake pressure is sampled in a similar way but every 15th degree instead.

**Estimator 1** Since the cylinder pressure is sampled at predetermined static angles on the crankshaft it is possible to compute the values for  $L(\theta)$ , Equation (3.2), at these angles beforehand and construct the corresponding vectors. The sampled in-cylinder pressures for each engine cycle, will come in 6 different vectors of 20 values each. Based on  $\theta$  the function selects the corresponding  $L(\theta)$  vector. The Reimann sum in Equation (3.11) is then calculated as a scaled sum of the scalar products between these vectors.

**Estimator 2** As mentioned in Section 4.5, Estimator 2 is sensitive to sensor drift. According to Volvo sources, the cylinder and intake manifold pressure should be approximately equal by the start of the combustion phase, i.e 180 degrees before TDC. The difference between the pressures at this point is used as an additive compensating term to correct for the drift.

The exhaust pressure, the intake manifold pressure as well as the drift compensating term is fed through moving average filters, based on values from previous engine cycles. The measurement vector,  $\tilde{y}$ , is then constructed together with the cylinder pressure at the angles decided in Section 4.4. Finally the scalar product according to Equation (3.16) is computed.

**Controller** The open loop control chain has been broken and the controllers have been inserted into the chain. A decision was made to insert the controllers early in the chain in order to protect as much of the pre-existing safety functionality as possible. The control function is executed once every engine cycle, in contrast with the estimator which is executed 6 times each engine cycle.

## 6.2 Engine test cell set-up

The test has been performed on a 13 litre diesel engine in a test cell at Volvo GTT. The engine has been equipped with a flush mounted pressure sensor from Kistler in the second cylinder. A suitable piezo-electric sensor amplifier from AVL called Microifem has been used to convert the charge generated by the sensor into a measurable voltage. The output range for the amplifier is 0 V - 10 V, therefore a voltage divider has been added to provide the range, 0 V - 5 V, that is used by the ECM. The amplifier also has a configurable input filter that has been set to 100kHz.

# 7 | Results

This chapter presents results from on-line testing of the functions. Data have been collected when running the estimators and controllers implemented on Volvo engine control hardware in an engine test cell. Since no other measurements of the indicated torque in the engine cell have been available no good reference data is available for comparison. Tests have therefore been conducted at the same operating points as is included in the data set, Appendix A, to be able to also compare the live estimate with simulated estimates on the data-set.

## 7.1 Torque estimation

Figure 7.1 displays the two estimators running at 4 different operating points,  $T_1$  -  $T_4$ .

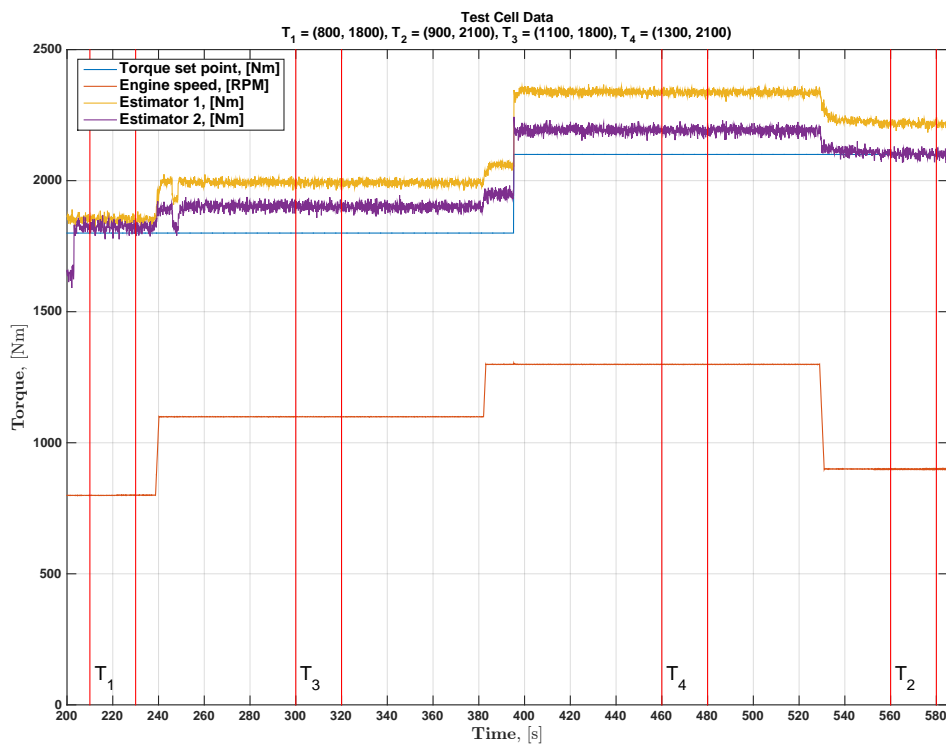
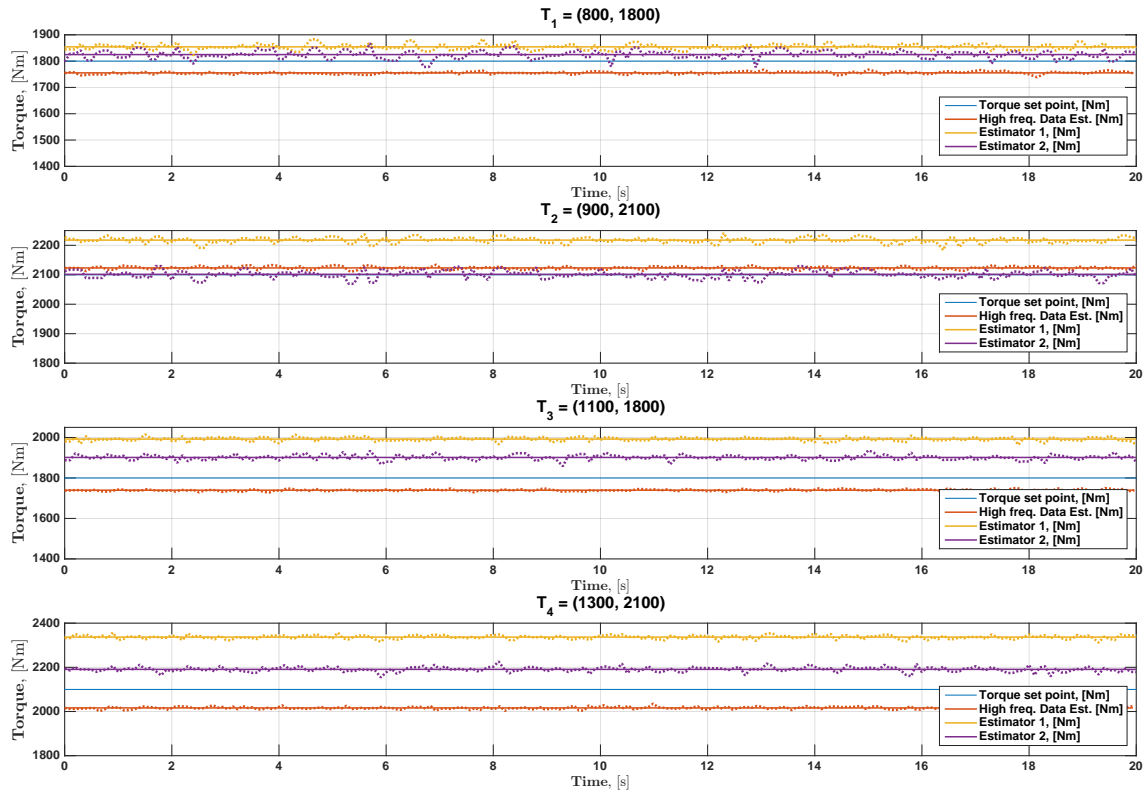


**Figure 7.1:** Test cell data: Estimator 1 and 2 running at different operating points. Steady-state data from interesting operating points are highlighted.

Data from these operating points have been used to assess the performance of the estimators by comparison to both the calibrated expected value (Torque set point)

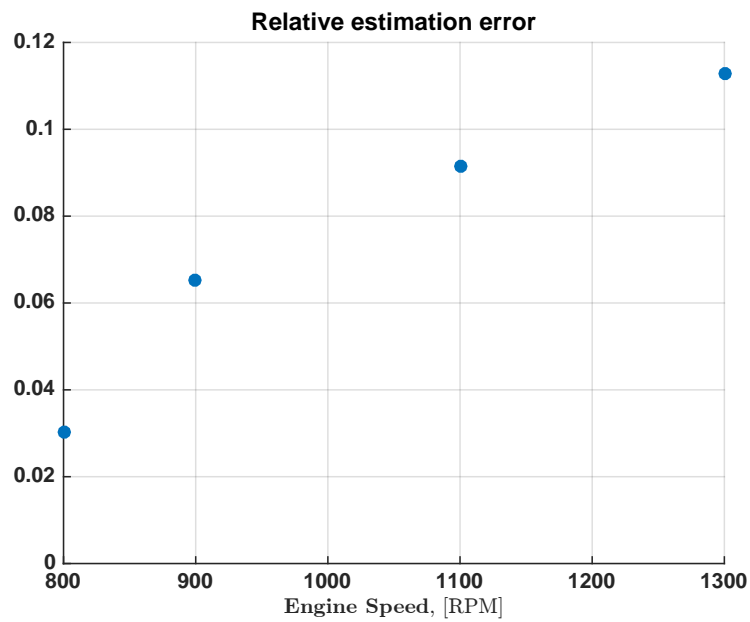
## 7. Results

and the best possible approximation using all data at the corresponding operating point in the high frequency sampled data set. Figure 7.2 displays this data.



**Figure 7.2:** Test cell data: Torque estimates from the two estimators and the two possible reference values. Both the signal (dotted) and the mean (solid) is plotted.

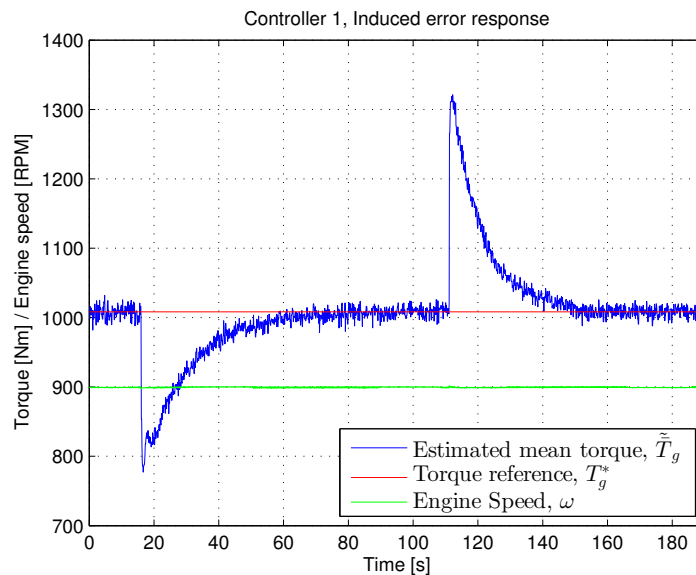
As can be seen in Figure 7.2 the two reference values differ a lot, the reference calculated using all data in the data-set tends to lie below the calibrated system reference. The two estimators tend to overestimate the indicated torque compared to both references and the size of the error seem to grow with increasing engine speed. Figure 7.3 shows the relative error of Estimator 1 when comparing with the calibrated system reference over engine speed.



**Figure 7.3:** *Relative error of Estimator 1 estimate compared to calibrated system reference plotted over engine speed.*

## 7.2 Closed loop torque controller 1

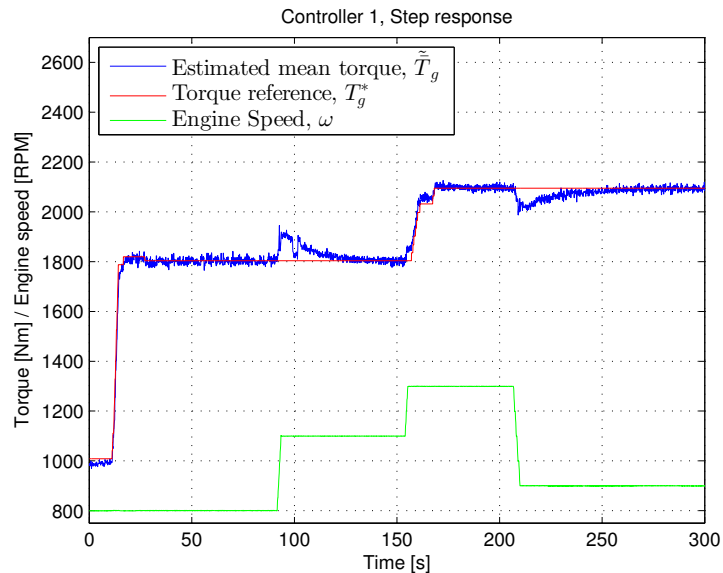
Figure 7.4 illustrate the behavior of the system when Controller 1 is used, here faulty injectors have been simulated by changing a software parameter.



**Figure 7.4:** *Illustration of the behavior of Controller 1 during simulated injection error. A fuel compensating factor for the injectors has been changed (twice) in order to simulate faulty injectors. The controller removes the error.*

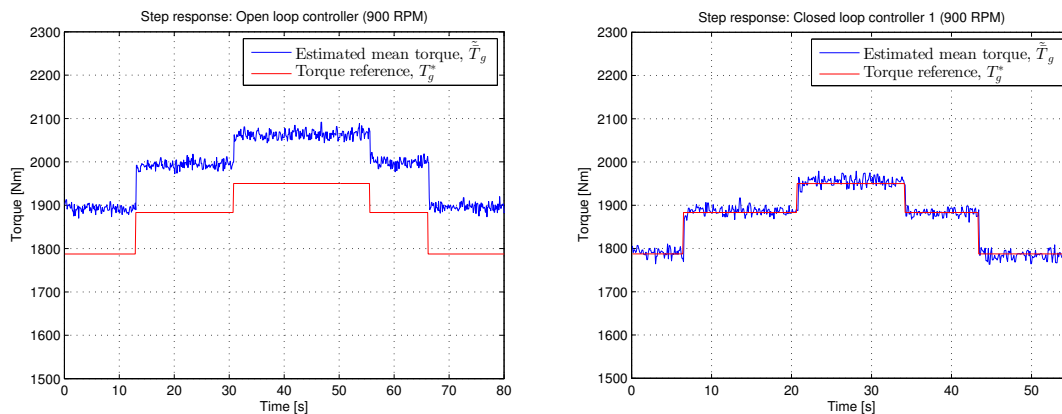
## 7. Results

Figure 7.5 and 7.6 shows the behavior of the system when switching between different operating points. For Figure 7.5 the engine has been set to run at the same operating points as used in Section 7.1.



**Figure 7.5:** The figure illustrate the behavior of Controller 1 when switching between the four different operating points used in Section 7.1.

Figure 7.7 illustrate the difference the conventional control structure and the closed loop control.



(a) Open loop control

(b) Closed loop Controller 1

**Figure 7.6:** Illustration of the difference in behavior when the closed loop control structure has been introduced. Engine speed is constant.

### 7.3 Closed loop torque controller 2

The assumption that motivates Controller 2 is that the control error at a specific operating point remains constant over time. The controller is meant to adapt its response and improve with time. This behavior is illustrated in Figure 7.7 where the reference switches between the same three operating points. The test demonstrates that the controller becomes more responsive and the error becomes lower as the time progresses.

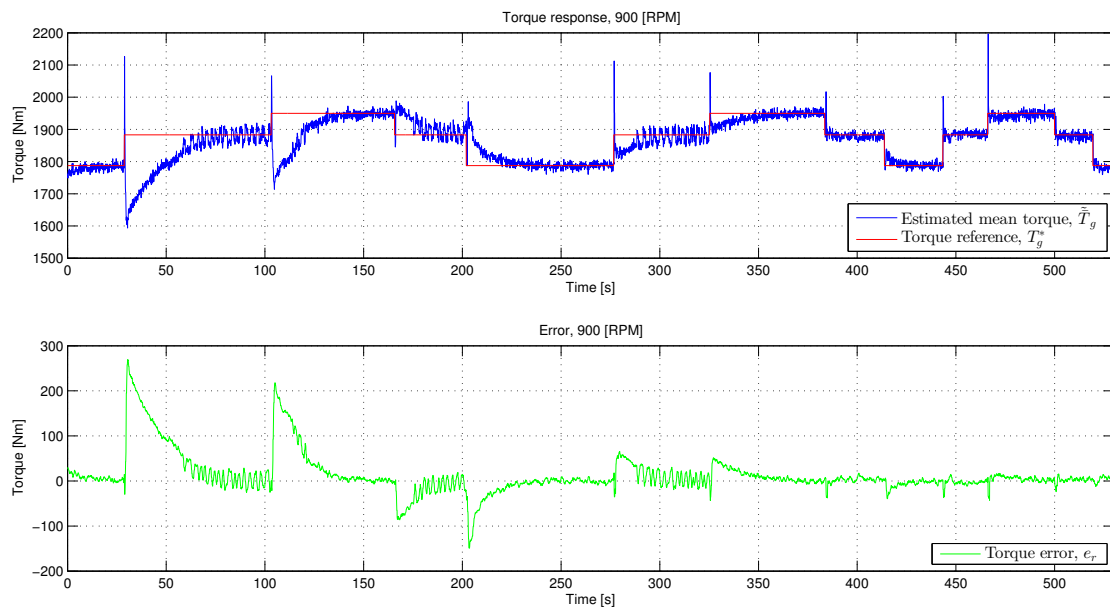


**Figure 7.7:** Output torque and error from Controller 2. Illustrates the controllers ability to adapt



# 8 | Discussion

In this chapter results from the engine cell tests and the different analyzes presented in Chapter 4 are discussed. First results from the estimation methods are addressed and then the implemented controllers.

## 8.1 Estimators

During this study it has not been possible to independently measure a reliable torque reference during testing of the estimation algorithms. What has been available instead is good measurements from a similar engine at the same operating points and the demanded indicated torque in the system, which should be reasonably close to the true torque.

When comparing the estimated torque with these two references, Figure 7.1, it is reasonable to expect some difference but impossible to know which is more correct. Assuming that the two references are closer to the true torque the estimators has considerable errors in their approximations. We see two possible sources for the error:

1. **Single sensor:** The assumption made in this study that the torque contribution from all the cylinders are approximately equal is questionable. As illustrated in Figure 4.4 the torque contributions from the different cylinders is considerable and introduces an uncertainty in the estimated value of approximately  $\pm 5\%$ . The reason that the estimator overestimates the torque could thus mean that the pressure in the cylinder where the sensor is placed is on average higher than in the others.
2. **Angular Offset:** Data presented in Figure 7.3 suggests that the error correlates well with the engine speed. Figure 7.6a also demonstrates that the error is close to constant when the engine speed is kept constant over different loads. Together, this suggests a constant time lag in the sampling of the in-cylinder pressure. If the lag is constant in time it would increase in angle with the rotational speed. As demonstrated in 4.6 the estimation methods are very sensitive to angular precision and the error increases linearly with the angular offset.

Both the simulations and the results from engine cell tests demonstrates a better result from Estimator 1 than that of Estimator 2. The motivation for Estimator 2, i.e. lower sampling frequency and thus also lower computational demand, is questionable. As demonstrated in Figure 4.5, the sampling frequency for Estimator 1 could be reduced down to 30 samples per cycle and still produce a better estimation than Estimator 2. When the sampling frequency for Estimator 1 has been reduced to this point, Estimator 1 uses 5 times the amount of data than Estimator 2. However, the drift compensating function of Estimator 2 must also be considered.

## 8.2 Controllers

The results demonstrates that closed loop control of indicated torque is possible. The two control strategies suggested in this study have different advantages. Both controllers seems to properly remove errors induced by faulty injectors. When switching between different operating points, as in Figure 7.5, it is hard to know how much the behaviour of the separately controlled engine break used in the test cell affects the behaviour of the controller showed in the plot. The controllers could possibly be made better and faster during these instances.

Because of the characteristics of the error sources, a controller similar to Controller 2 would likely be what is finally implemented into production type engines. Figure 7.7 illustrates the advantage of this type of controller when correcting for these types of errors. Improvements to Controller 2 can be made. One improvement suggested for Controller 2 is to introduce logic that dictates under which conditions the dynamic look-up table should be updated, steady state operation would be one such condition.

## 9 | Conclusion

The use of a single in-cylinder pressure sensor to estimate the average indicated torque of a heavy duty diesel engine have been studied in this thesis. Two methods for on-line estimation of the average indicated torque has been tested and analyzed. The study has showed that the angular precision when sampling the cylinder pressure is very important for the accuracy of the estimation but that the sampling interval can be moderate and still produce a compelling result. The in-cylinder pressure sensors usually drifts over time. The impact of this drift can in one of the methods be neglected without affecting the estimation. It was assumed that the torque contribution from all cylinders was approximately equal, motivating the use of only a single ICPS. Analysis of test data showed that this assumption may induce an error of approximately  $\pm 5\%$  in the total torque estimation.

When the methods were evaluated on a test cell engine the estimated value differed from the available references with around 10% at maximum. This difference could be explained by the fact that the available references also are only estimates and by the error margin introduced when using only one sensor. The test data also suggests the presence of a time lag in the sampling of the pressure which would give an error in the estimation. To further investigate the size and cause of the assumed error a separately measured and more accurate reference would be needed.

Closed loop torque control with torque estimation as feedback has also been studied in this thesis. By using a simple integrating controller it was demonstrated that an indicated torque error introduced by faulty/worn injectors could be effectively removed. The first controller was then extended with a dynamic look-up table that is populated by the integrated errors from different operating points. The second controller showed promising result when the engine switches between different operating points.

Overall the study has showed that estimating the average indicated torque for control purposes is a feasible application for in-cylinder pressure sensors in production type engines.



# 10 | Future Work

This chapter presents some possible improvements to the study and gives some suggestion on how the work conducted in this thesis could be continued.

## 10.1 Gather reference data and analyze error

As discussed it has not been possible during this study to independently measure a good average torque reference during the cell tests. Thus the error in the live estimates have been hard to analyze. Running more cell tests and measure a good reference need to be done to be able to analyze the source of the error further. If this analysis also point to a time-lag in the sampling a simple addition to the algorithm that compensates for this should be possible to implement.

## 10.2 Adaptive reference feed forward controller

For the adaptive controller proposed in Chapter 5 (Controller 2) the error is modeled as a disturbance. Another way of thinking about the error is to view it as a model error. With the system still considered as static this would mean that  $G(z)$  is not equal to one anymore but some other gain,  $\hat{G}(z)$ .

It then make sense to stop focusing on the feedback but instead trying to adapt the reference feed-forward,  $F_r(z)$ . The feedback can then be kept like implemented in Controller 1.

## 10.3 Individually weighting cylinder contributions

As presented in Chapter 3, the assumption that the pressure-angle relationship in all cylinders are equal was made. Thus the contribution from all cylinders are being weighted equally. Analysis of this assumption have shown that this could yield an error of up to 5%. It may be possible to reduce this error by individually weighting the contribution of the not measured cylinders with a factor calculated from other measurements.

The total average indicated torque is expressed in terms of one measured pressure,  $p_{g,x}(\theta)$  as

$$\bar{T}_g = \sum_{i=1}^{N_c} w_i \bar{T}_{g,x}, \quad (10.1)$$

where  $w_i$  are weights relating torque contribution in different cylinders to that of cylinder  $x$ ,  $w_x = 1$ . Algorithms using momentaneous engine speed measurements to calculate the weights have been developed with promising results [5]. Depending on

the quality of the momentaneous engine speed measurements over the cycle it may be possible to reduce the error using such an approach.

### **10.4 Investigating impact of crankshaft torsion on estimation accuracy**

Torque is being applied on the crankshaft at the positions of the 6 cylinders and a load torque is applied at the output side of the shaft. The crankshaft is not completely stiff and considering the sensitivity to angular precision in pressure measurements of the estimation methods torsion of the crankshaft may impact the precision of the estimation.

The distance on the crankshaft between the pressure measurements and the angle measurements depends on from which cylinder we choose to measure pressure. In the current implementation, pressure is measured in cylinder 2, quite far from the flywheel where the angle is measured. The torque applied on the shaft will twist the shaft between the two points of measure and this will give a varying angular error over the cycle. How large the impact of this torsion is at different operating points can be estimated through dynamic simulations of the crankshaft response to applied torques at these operating conditions and including the resulting angular deviations in the estimation algorithms.

# Bibliography

- [1] A. Guzzella and C. Onder. *Introduction to Modeling and Control of Internal Combustion Engine Systems*. Springer, 1st edition, 2004.
- [2] Marcus Hedegård. *Estimation of Torque in Heavy Duty Vehicles with Focus on Sensor Hysteresis*. PhD thesis, Chalmers University of Technology, 2016. ISBN: 978-91-7597-471-2.
- [3] J.B. Heywood. *Internal combustion engine fundamentals*. Mcgraw-hill, 1988.
- [4] U. Kiencke and L. Nielsen. *Automotive Control Systems*. Springer, 2nd edition, 2005.
- [5] M. Kyunghan, C. Jaesung, K. Eunhwan, and S. Myoungho. Individual cylinder imep estimation using a single cylinder pressure sensor for light-duty diesel engines. *SAE Technical Paper 2014-01-1347*, 2014. doi:10.4271/2014-01-1347.
- [6] S. Larsson and S. Schagerberg. Si-engine cylinder pressure estimation using torque sensors. *SAE Technical Paper 2004-01-1369*, 2004. doi:10.4271/2004-01-1369.
- [7] Alan J. Laub. *Matrix Analysis for Scientists Engineers*. Society for Industrial Applied Mathematics, 1st edition, 2005.
- [8] Paul A. Battiston Mark C. Sellnau, Frederic A. Matekunas and David R. Lancaster Chen-Fang Chang. Cylinder-pressure-based engine control using pressure-ratio-management and low-cost non-intrusive cylinder pressure sensors. *SAE Technical Paper 2000-01-0932*, 2000. doi:10.4271/2000-01-0932.
- [9] S Milton and J Arnold. *Introduction to Probability and Statistics: Principles and applications for engineering and the computing sciences*. McGraw-Hill, 4th edition, 2003.
- [10] D. Moser, S. Hahn, H. Waschl, and Luigi del Re. Torque control of a diesel engine by an eigenpressure based approach. *Control Conference (ECC), 2013 European*, 2013. ISBN: 978-3-033-03962-9.
- [11] U.S. Department of Energy. Alternative fuels data center - fuel properties comparison. [https://www.afdc.energy.gov/fuels/fuel\\_comparison\\_chart.pdf](https://www.afdc.energy.gov/fuels/fuel_comparison_chart.pdf), 2014. Last visited: 2017-06-12.
- [12] Gregg W. Pestana. Engine control methods using combustion pressure feedback. *SAE Technical Paper 890758*, 1989. doi:10.4271/890758.
- [13] S. Schagerberg and T. McKelvey. Instantaneous crankshaft torque measurements - modeling and validation. *SAE Technical Paper 2003-01-0713*, 2003. doi:10.4271/2003-01-0713.

- [14] Steven W. Smith. *The Scientist Engineer's Guide to Digital Signal Processings*. California Technical Publishing, 2nd edition, 1999.
- [15] L. Taalman and P. Kohn. *Calculus*. W.H. Freeman and Company, 2nd edition, 2014.
- [16] Mikael Thor. *Torque based combustion property estimation and control for diesel engines*. PhD thesis, Chalmers University of Technology, 2012. ISBN: 978-91-7385-705-5.
- [17] B. Varoquie, A. Hellemans, A. Pournain, D. Heinitz, and C. Bourquey. Sia powertrain - rouen 2016. In *ICPS based Combustion Control: An efficient way to reduce engineering margin for Diesel engines*, 2016.

# A | Appendix 1

ID	RPM	Nm	$n_s$	$f_s$ [Hz]	$f_\theta$ [ $\frac{1}{\theta}$ ]	$n_T$
1	800	1800	1591244	51200	10.67	207
2	800	2100	1564625	51200	10.67	204
5	900	1800	1744859	51200	9.48	256
6	900	2100	1572837	51200	9.48	230
7	900	2350	1581046	51200	9.48	232
8	900	2650	1626098	51200	9.48	238
9	1000	1800	1587173	51200	8.53	258
10	1000	2100	1589228	51200	8.53	259
11	1000	2350	1593316	51200	8.53	259
12	1000	2650	1906680	51200	8.53	310
13	1100	1800	1552381	51200	7.76	278
14	1100	2100	1574888	51200	7.76	282
15	1100	2350	1587194	51200	7.76	284
16	1100	2650	1591276	51200	7.76	285
17	1200	1800	1613801	51200	7.11	315
18	1200	2100	1589228	51200	7.11	310
19	1200	2350	1548280	51200	7.11	302
20	1200	2650	1587197	51200	7.11	310
21	1300	1800	2564081	51200	6.56	543
22	1300	2100	1591276	51200	6.56	337
23	1300	2350	1578987	51200	6.56	334
24	1300	2650	1578992	51200	6.56	334
25	1400	1800	2623479	51200	6.10	598
26	1400	2100	1535986	51200	6.10	350
27	1400	2350	1568753	51200	6.10	357
28	1400	2650	1605619	51200	6.09	366
29	1500	1800	1597430	51200	5.69	390
30	1500	2100	2416630	51200	5.69	590
31	1500	2350	1595378	51200	5.69	390
32	1500	2650	1613802	51200	5.69	394
33	1600	1800	1654774	51200	5.33	431
34	1600	2100	2031597	51200	5.33	529
35	1600	2350	1597428	51200	5.33	416
36	1600	2650	1591284	51200	5.33	414
37	1700	1800	1566712	51200	5.02	434
38	1700	2100	1640426	51200	5.02	454
39	1700	2350	1603568	51200	5.02	444
40	1700	2650	1615862	51200	5.02	447
41	1800	1800	1585141	51200	4.74	464
42	1800	2100	1601519	51200	4.74	469
43	1800	2350	1605623	51200	4.74	470
44	1800	2650	1564661	51200	4.74	458

**Table A.1:** Data set,  $n_s$ : number of samples,  $f_\theta$ : approximate sampling frequency in angle,  $n_T$ : approximate number of full engine cycles